Soil resource acquisition strategy modulates global plant nutrient and water economics

Alissar Cheaib (iD), Jeff Chieppa, Evan A. Perkowski (iD) and Nicholas G. Smith (iD)

Department of Biological Sciences, Texas Tech University, Lubbock, TX 79409, USA

Summary

• Natural selection favors growth by selecting a combination of plant traits that maximize photosynthetic CO_2 assimilation at the lowest combined carbon costs of resource acquisition and use. We quantified how soil nutrient availability, plant nutrient acquisition strategies, and aridity modulate the variability in plant costs of nutrient acquisition relative to water acquisition (β).

• We used an eco-evolutionary optimality framework and a global carbon isotope dataset to quantify β.

• Under low soil nitrogen-to-carbon (N : C) ratios, a mining strategy (symbioses with ectomycorrhizal and ericoid mycorrhizal fungi) reduced β by mining organic nitrogen, compared with a scavenging strategy (symbioses with arbuscular mycorrhizal fungi). Conversely, under high N : C ratios, scavenging strategies reduced β by effectively scavenging soluble nitrogen, compared with mining strategies. N_2-fixing plants did not exhibit reduced β under low N : C ratios compared with non-N_2-fixing plants. Moisture increased β only in plants using a scavenging strategy, reflecting direct impacts of aridity on the carbon costs of maintaining transpiration in these plants. Nitrogen and phosphorus colimitation further modulated β.

• Our findings provide a framework for simulating the variability of plant economics due to plant nutrient acquisition strategies in earth system models.

Introduction

A quantitative understanding of how plants acquire and allocate resources such as carbon, water, and nutrients is crucial for predicting their fitness in diverse environments (Mooney, 1972) and for forecasting terrestrial ecosystem responses to environmental changes (Rogers *et al.*, 2017; Crowther *et al.*, 2019; Smith & Keenan, 2020). Plant strategies for acquiring soil nutrients and water significantly influence carbon gain (e.g. photosynthetic capacity) and plant growth (Chapin III *et al.*, 1993; Farquhar *et al.*, 2002), yet these strategies also necessitate the allocation of photosynthates to belowground processes, imposing a carbon cost to the plant (Högberg *et al.*, 2008, 2010; Drigo *et al.*, 2010; Raich *et al.*, 2014; Gill & Finzi, 2016; Shi *et al.*, 2016). Indeed, uncertainties in earth system models (ESMs) regarding future land carbon budgets often arise from how these models represent these carbon costs (Braghiere *et al.*, 2022).

Nitrogen (N) and phosphorus (P) are essential and often limiting nutrients for plant growth and terrestrial ecosystem net productivity (Güsewell, 2004; Elser *et al.*, 2007; Lambers *et al.*, 2008; LeBauer & Treseder, 2008; Vitousek *et al.*, 2010; Harpole *et al.*, 2011; Yuan & Chen, 2012; Turner *et al.*, 2018; Du *et al.*, 2020). Given their various forms in soils (Vitousek & Howarth, 1991; Vitousek *et al.*, 2010), plants have evolved diverse nutrient acquisition strategies involving belowground

carbon allocation to mobilize and take up these nutrients (Gutschick, 1981; Vance *et al.*, 2003; Hodge & Storer, 2015). Broadly speaking, root nutrient acquisition includes nonsymbiotic strategies (Chapman *et al.*, 2012) and symbiotic strategies, such as associations with mycorrhizal fungi (Smith & Read, 2010; van Der Heijden *et al.*, 2015) and N_2-fixing bacteria (Vance & Heichel, 1991; Udvardi & Poole, 2013).

Nonsymbiotic strategies involve nutrient mobilization and uptake by roots through diffusion and mass flow (Dekker & Ritsema, 1996; Jungk, 2001), particularly when soluble forms are near the root zone (Barber, 1962, 1995). They also include the release of carboxylates and phosphatases to solubilize bound P, especially in plants with specialized cluster roots (Lambers *et al.*, 2006, 2008; Raven *et al.*, 2018), and the secretion of root exudates to stimulate soil microbial communities (Phillips *et al.*, 2011; Wen *et al.*, 2022). Most vascular plants form symbioses with mycorrhizal fungi, with only 8% being nonmycorrhizal (NM; Brundrett, 2009; Brundrett & Tedersoo, 2018). These fungi form external mycelial networks that extend beyond root depletion zones, exploring large soil volumes for nutrient acquisition (Smith & Read, 2010; Shi *et al.*, 2023) and water uptake (Duddridge *et al.*, 1980; Querejeta *et al.*, 2003, 2006; Augé *et al.*, 2004; Allen, 2007; Lehto & Zwiazek, 2011; J. Wang *et al.*, 2021; Kakouridis *et al.*, 2022; Castaño *et al.*, 2023). These resources are delivered to the roots in exchange for plant
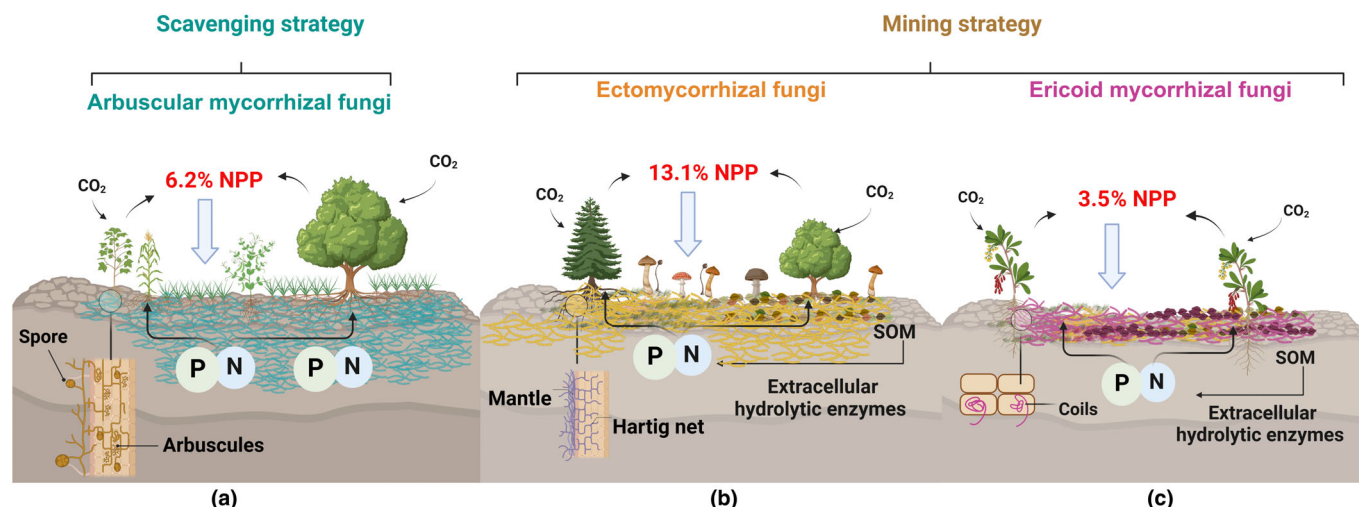
Fig. 1 Illustration depicting various symbioses with mycorrhizal fungi employing distinct nutrient acquisition strategies: (a) mycorrhizal fungi using a scavenging strategy include arbuscular mycorrhizal fungi (AMF) and are estimated to receive *c.* 6.2% of a plant's total net primary productivity (NPP) (Hawkins *et al.*, 2023). Mycorrhizal fungi using a mining strategy include (b) ectomycorrhizal fungi (EcMF), which are estimated to receive *c.* 13.1% of a plant's total NPP (Hawkins *et al.*, 2023), and (c) ericoid mycorrhizal fungi (ErMF), which are estimated to receive *c.* 3.5% of a plant's total NPP (Hawkins *et al.*, 2023). The extensive extraradical mycelium of mycorrhizal fungi expands the root system's surface area-to-volume ratio, enhancing the fungi's capacity to scavenge soluble inorganic forms of nutrients and absorb water. The tree-like arbuscular structures and coils of AMF formed by intraradical hyphae within root cortical cells facilitate the transfer of these resources to root cells (van Der Heijden *et al.*, 2015; Bennett & Groten, 2022). EcMF hyphae also proliferate extensively in nutrient-rich patches (Leake *et al.*, 2004; Allen, 2007; Raven *et al.*, 2018; See *et al.*, 2022). Several species of EcMF and ErMF possess a high capacity to produce extracellular hydrolytic enzymes that decompose soil organic material and release N and P from insoluble organic complexes (Phillips & Fahey, 2006; Brzostek & Finzi, 2011; Phillips *et al.*, 2013; Yin *et al.*, 2014; Midgley & Phillips, 2019). See Table 1 for more details. This figure was created in BioRender (Cheaib, A. (2025) https://BioRender.com/a59z835).

photosynthates, including carbohydrates and lipids (Högberg *et al.*, 2008; Bennett & Groten, 2022). Consequently, mycorrhizal symbioses are fundamental to plant water and carbon dynamics, with mycorrhizal fungi serving as a significant sink for plant-assimilated carbon (Treseder & Allen, 2000; Hawkins *et al.*, 2023), receiving 4–20% of a plant's total net primary productivity (NPP) (Koch & Johnson, 1984; Douds *et al.*, 1988; Hawkins *et al.*, 2023). However, this allocation varies widely, influenced by a myriad of factors, such as climate, soil nutrient availability, texture and moisture (Chen *et al.*, 2014; Terrer *et al.*, 2016, 2018; Ledo *et al.*, 2018; Hartmann *et al.*, 2020; Perkowski *et al.*, 2021, 2024), and mycorrhizal functional group (Fig. 1; Hawkins *et al.*, 2023).

Depending on the soil substrate from which mycorrhizal fungi extract N and P, they can be categorized into two major functional groups (Lambers *et al.*, 2008): those employing a scavenging strategy, primarily arbuscular mycorrhizal fungi (AMF) (Table 1; Fig. 1a), and those employing a mining strategy, mainly ectomycorrhizal fungi (EcMF) (Table 1; Fig. 1b) and ericoid mycorrhizal fungi (ErMF) (Table 1; Fig. 1c). Both AMF and EcMF have extensive extraradical mycelia that expand the root system's surface area-to-volume ratio, enhancing their ability to 'scavenge' soluble nutrients and absorb water (Fig. 1a,b; van Der Heijden *et al.*, 2015; Bennett & Groten, 2022; Leake *et al.*, 2004; Allen, 2007; See *et al.*, 2022). However, AMF have a limited capacity to mobilize nutrients from insoluble organic complexes containing N and P (Lambers *et al.*, 2008), whereas many EcMF and ErMF (collectively EEMF) produce

extracellular hydrolytic enzymes that break down soil organic material, enabling nutrient mining (Phillips & Fahey, 2006; Brzostek & Finzi, 2011; Phillips *et al.*, 2013; Yin *et al.*, 2014; Midgley & Phillips, 2019). Since AMF rely more on scavenging soluble nutrients, we categorized them under the scavenging strategy, while EEMF, which are more effective in mining nutrients from insoluble organic complexes, were categorized under the mining strategy.

Moreover, certain angiosperms, such as 'rhizobial' legumes and 'actinorhizal' species, form symbiotic relationships with N_2-fixing bacteria (Pawlowski & Newton, 2007). These bacteria form specialized root nodules (Lindström & Mousavi, 2020) that reduce atmospheric N_2 to ammonia and are considered the primary natural nitrogen source for the terrestrial biosphere (Udvardi & Poole, 2013; Vitousek *et al.*, 2013). However, like mycorrhizal associations, this symbiosis incurs a carbon cost, requiring 4–16% of the plant's photosynthetically assimilated carbon to maintain nodule formation (Finke *et al.*, 1982; Kaschuk *et al.*, 2009, 2010).

Some ESMs have begun to quantify these soil resource acquisition costs explicitly by incorporating nitrogen fixation and uptake (Fisher *et al.*, 2010), carbon–nitrogen trade-offs associated with mycorrhizal fungi (Brzostek *et al.*, 2014) and, more recently, P dynamics (Raven *et al.*, 2018; Allen *et al.*, 2020). Quantifying these costs has proven to be crucial for refining global carbon cycle models (Braghiere *et al.*, 2022). However, a global framework that accounts for how these costs vary with soil nutrient availability and climatic factors, while also considering

Table 1 Characteristics of the main mycorrhizal fungal symbioses analyzed in this study.

Characteristics of the main mycorrhizal fungal symbioses analyzed in this study

AMF	*Description*: Arbuscular mycorrhizal fungi (AMF): symbiotic associations between Glomeromycota fungi and the roots of *c*. 70% of land plants (Smith & Read, 2010). AMF evolved in early land plants and are globally distributed, covering 55% of global vegetation (Soudzilovskaia *et al*., 2019), with the highest density in the subtropics (Barceló *et al*., 2023). AMF hyphae penetrate the outer root cell layers and form coils and arbuscules in the cortical cells, which are the primary sites for nutrient exchange (Fig. 1a) (Tedersoo & Bahram, 2019).
	Nutrient acquisition: AMF are obligate symbionts with limited saprophytic abilities, meaning they cannot decompose soil organic matter (SOM; Phillips *et al*., 2013). However, their mycelia quickly colonize soil patches rich in inorganic nitrogen and phosphorus, efficiently scavenging and transferring these nutrients to host plants (Marschner & Dell, 1994; Hawkins *et al*., 2000).
	Plant hosts: Various plant growth forms (woody, herbaceous, forbs, and crop species) and phylogenetic groups (primarily angiosperms such as ash and maples, many tropical tree species, and some gymnosperms such as cedars and redwoods)
EcMF	*Description*: Ectomycorrhizal fungi (EcMF) symbiotically associate with the roots of *c*. 2% of land plants, involving Basidiomycota, Ascomycota, and Mucoromycota fungi (Tedersoo & Smith, 2013). Found in tropical, temperate boreal regions, EcMF are most abundant in the latter, covering 25% of vegetation (Martin *et al*., 2016). Evolved multiple times over 200 million years, EcMF form a mycelial mantle around root tips, including a Hartig net, for carbon–nutrient exchange (Fig. 1b) (Brundrett & Tedersoo, 2018).
	Nutrient acquisition: EcMF are facultative plant symbionts, some possess saprophytic abilities, producing hydrolytic and oxidative enzymes that decompose SOM (Fig. 1b). This capability allows EcMF to access nitrogen and phosphorus from organic pools that are usually inaccessible to AMF (Read & Perez-Moreno, 2003; Phillips *et al*., 2013).
	Plant hosts: Primarily woody gymnosperms and angiosperms in boreal and temperate forests, and some tropical forest trees.
ErMF	*Description*: Ericoid mycorrhizal fungi (ErMF) are symbiotic associations between Ascomycota and Basidiomycota fungi and the roots of Ericaceae plants (Vohník, 2020). Less than 1% of plants have ErM associations, covering under 3% of global vegetation, and present in all continents except Antarctica (Kohout, 2017).
	Nutrient acquisition: ErM hyphae form coils inside the fine roots of ericaceous plants found in acidic and infertile soils (Fig. 1c). Like EcMF, they can also produce extracellular hydrolytic enzymes (Bending & Read, 1997).
	Plant hosts: Ericaceae

photosynthetic acclimation processes, could offer an alternative approach to estimating them.

At the individual species level and leaf scale, the least-cost hypothesis, a subset of eco-evolutionary optimality (EEO) theory (Franklin *et al*., 2020; Harrison *et al*., 2021), provides a framework that links photosynthetic acclimation to the carbon costs of nutrient acquisition relative to water acquisition (Wright *et al*., 2003; Prentice *et al*., 2014; Wang *et al*., 2017a; Querejeta *et al*., 2022), and this integrative approach has already been successfully incorporated into some land surface models (Smith *et al*., 2019; Qiao *et al*., 2020; Stocker *et al*., 2020; Mengoli *et al*., 2022). EEO principles suggest that plants have evolved soil resource acquisition strategies that minimize acquisition costs while maximizing resource uptake (Franklin *et al*., 2020; Harrison *et al*., 2021). Within this framework, the photosynthetic least-cost hypothesis posits that water and nutrients are resources that can be substituted to maximize light use for photosynthetic carbon assimilation (Wright *et al*., 2003). Assuming all other factors are constant, photosynthesis can be maximized either through increased investment in photosynthetic enzymes, which require nutrients, or by allowing greater stomatal conductance to CO_2, which requires water (Paillassa *et al*., 2020; Querejeta *et al*., 2022). Balancing investments between water transport capacity and nutrient-rich photosynthetic enzymes leads to an optimal ratio of the CO_2 concentration in the substomatal cavities (C_i) to ambient CO_2 concentration (C_a) (Field, 1986; Franks & Brodribb, 2005). Consequently, the $C_i : C_a$ ratio emerges as a pivotal functional trait for the coupling of transpiration and photosynthesis and is thought to be optimized to a given environment through acclimation and adaptation (Prentice *et al*., 2014; Paillassa *et al*., 2020; Querejeta *et al*., 2022).

The EEO framework has proven to be effective in predicting the acclimation of a variety of photosynthetic traits, including the maximum rate of ribulose-1,5-bisphosphate carboxylase/oxygenase (RuBisCO) carboxylation (V_{cmax}) (Smith *et al*., 2019), stomatal conductance (Cowan & Farquhar, 1977; Sperry *et al*., 2017), and the optimal $C_i : C_a$ ratio, referred to as χ hereafter (Prentice *et al*., 2014; Wang *et al*., 2017a,b; Lavergne *et al*., 2020). The complete derivation of an optimally acclimated χ involves a ratio that links soil resources to leaf-level acclimation (Prentice *et al*., 2014; Wang *et al*., 2017a,b; Paillassa *et al*., 2020):

$$\beta = b_\beta / a_\beta$$

where b_β represents the carbon cost of acquiring nutrients and maintaining photosynthetic enzymes to support carboxylation, and a_β represents the carbon cost of acquiring water and maintaining water transport to support assimilation at the same rate (Prentice *et al*., 2014; Wang *et al*., 2017a,b; Paillassa *et al*., 2020).

The ratio 'β' is often assumed to be constant in land surface model implementations of the theory (e.g. Qiao *et al*., 2020; Stocker *et al*., 2020; Mengoli *et al*., 2022) due to the lack of a predictive framework for its variability. However, soil nutrient availability and moisture levels are highly variable and interdependent in natural conditions. The term b_β is expected to decrease with increasing soil nutrient availability, as the investment required for nutrient acquisition diminishes. Similarly, the term a_β is expected to decrease with increasing moisture, as water uptake and transport investments are reduced with increasing water availability (Paillassa *et al*., 2020). These terms are also expected to covary, interact, and be influenced by the complex interplay between moisture, nutrient forms, and nutrient acquisition strategies.
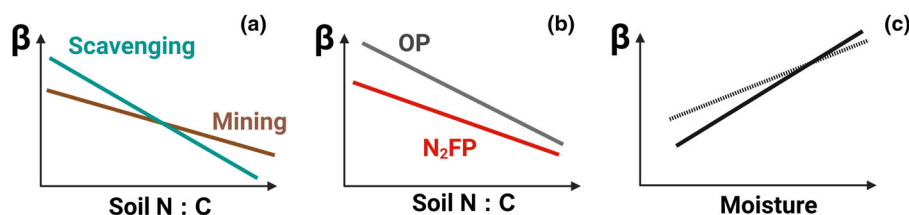
Fig. 2 Schematic representation of the hypotheses proposed regarding the variability of the carbon costs of nutrient acquisition relative to water acquisition (β) in response to (a and b) soil nitrogen-to-carbon (N : C) ratios, as well as (c) moisture, depending on nutrient acquisition strategies. The carbon costs of nutrient acquisition relative to water acquisition (β) are expected to decrease with increasing soil N : C ratios, as the investment in nutrient acquisition to achieve a given amount of nutrient uptake is reduced with increasing N availability in soils. (a) The mining strategy is expected to be less energetically costly for acquiring nutrients relative to water under low soil N : C ratios compared with the scavenging strategy. Conversely, this trend is anticipated to reverse under high N : C ratios. (b) N_2-fixing plants (N_2FP) are expected to exhibit lower costs of nutrient acquisition relative to water acquisition, particularly at low soil N availability, compared to other plants (OP). In N_2FP, the carbon costs of nutrient acquisition relative to water acquisition are expected to converge with OP as N availability increases. This is because, with higher nutrient availability, plants typically invest less in energy-intensive N_2-fixation pathways and shift toward more efficient direct uptake mechanisms. (c) The carbon costs of nutrient acquisition relative to water acquisition (β) are predicted to increase with increasing moisture levels, as water availability reduces the investment required for water uptake and transpiration (straight line). However, low MI is expected to directly decrease nutrient availability and uptake. To compensate for this decrease, plants are expected to increase the carbon costs of nutrient acquisition ($b_β$), and consequently increasing β (dashed line) relative to the case where low MI may not impact $b_β$. Created in BioRender. Cheaib, A. (2025) https://BioRender.com/k81o451.

Some studies have explored the impact of soil water availability on β and found that β decreases with reduced plant-available soil water (Stocker *et al.*, 2018), attributed primarily to an increasing cost of water transport $a_β$ along the soil–plant–atmosphere continuum (Lavergne *et al.*, 2020). However, limited attention has been given to assessing β variability based on the interactions between soil nutrient availability, aridity, and plant nutrient acquisition strategy. That is why we aimed to evaluate how β varies with these factors. To achieve this, we compiled a global dataset of available leaf carbon isotope measurements to calculate χ and estimate β from χ (see the Materials and Methods section).

Starting with the most straightforward expectations, one might predict that increasing moisture would increase the carbon costs of nutrient acquisition relative to water acquisition (β) due to a decrease in the carbon cost of water uptake and transpiration, $a_β$. Similarly, increasing soil nutrient availability should decrease β, as a result of a decrease in the carbon cost of nutrient acquisition, $b_β$. However, the reality is far more complex. These expected variations depend on interactions with nutrient acquisition strategies, N and P colimitation, and the influence of moisture on soil nutrient forms, availability, and uptake. Thus, based on contemporary, well-accepted paradigms predicting that plants will preferentially allocate carbon to acquire the most limiting resource (Valentine & Mäkelä, 2012; McMurtrie & Dewar, 2013), we introduced additional processes to refine these expectations and proposed the following hypotheses:

H1: *In areas with low soil nitrogen-to-carbon (N : C) ratios, a mining strategy (symbioses with EEMF; Table 1; Fig. 1b,c) will reduce the carbon costs of nutrient acquisition relative to water acquisition (β) compared with a scavenging strategy (symbiosis with AMF) (Fig. 2a). This is because EEMF can 'mine' insoluble N from soil organic materials, whereas AMF have limited ability to do so. Conversely, in areas with high soil N : C ratios, a scavenging strategy*

is expected to reduce β compared with a mining strategy (Fig. 2a), as AMF primarily 'scavenge' soluble N.

H2: *As soil N availability decreases, plants with N_2-fixing bacteria (N_2-fixing plants, N_2FP hereafter) will exhibit reduced nutrient acquisition costs relative to water acquisition (β) compared with plants without such associations (other plants, OP hereafter) (Fig. 2b). This hypothesis is based on the observation that N_2-fixation is less costly than direct N uptake in low-N environments (Rastetter et al., 2001; Perkowski et al., 2024) and that plant investments in symbiotic N_2-fixing bacteria generally decrease with increasing soil N availability as roots can directly take up N at lower investment cost (Rastetter et al., 2001; Terrer et al., 2016, 2018; Perkowski et al., 2021).*

H3: *For both scavenging and mining strategies, increasing moisture should increase the carbon costs of nutrient acquisition relative to water acquisition (β) due to a decrease in the cost for acquiring water and maintaining transpiration ($a_β$) (Fig. 2c). However, aridity should also directly affect nutrient availability (Finzi et al., 2011; Delgado-Baquerizo et al., 2013, 2018; Hou et al., 2018) and uptake (McMurtrie & Näsholm, 2018). Under arid conditions, reduced transpiration could impair soluble nutrient uptake via mass flow and diffusion (Nye, 1977; Gerber et al., 2010; Oyewole et al., 2014; Joseph et al., 2021). Therefore, depending on the degree to which nutrient uptake and availability are reduced, plants would be expected to increase carbon allocation belowground to compensate, thereby increasing the carbon costs of acquiring nutrients ($b_β$). This could increase β under arid conditions (Fig. 2c).*

H4: *The carbon costs of nutrient acquisition relative to water acquisition (β) are expected to decrease as plant-available inorganic soluble phosphorus concentrations (P_i) increase, regardless of whether a mining or scavenging strategy is employed. However, this prediction may be complicated by N and P colimitation and*

interactions with moisture. In ecosystems primarily limited by N, in which N and P are mainly sequestered in insoluble organic forms, such as in temperate and boreal forests (Hyvönen et al., 2007), β may depend more on the soil N : C ratio than on P_i availability. By contrast, in ecosystems where N and P are colimited, such as some tropical and subtropical ecosystems with old, P_i-impoverished soils (Lambers et al., 2008; Vitousek et al., 2010; Soudzilovskaia et al., 2015; Vallicrosa et al., 2022), β may be influenced by both the soil N : C ratio and P_i. Additionally, in these regions, where P and N forms are predominantly inorganic due to higher mineralization rates (Marklein et al., 2016), aridity's interaction with soluble nutrients may further complicate predictions, potentially altering how β varies with P_i.

Materials and Methods

We calculated χ using global datasets of leaf stable carbon isotope (δ¹³C, ‰) measurements spanning the period 1830–2018. We used these isotope-derived χ values ($\chi_{isotopes}$) to calculate β for each sample (will be discussed later). The dataset includes sites distributed globally, covering various biomes (Supporting Information Figs S1, S2), and includes leaves from species known to associate with different types of microbial symbionts.

Observational dataset of δ¹³C and plant nutrient acquisition strategies

We aggregated six compilations of leaf δ¹³C data from vascular plants in natural and seminatural habitats, encompassing a total of 501 samples from Diefendorf et al. (2010), 845 samples from Sheldon et al. (2020), 3979 samples from Cornwell et al. (2018), 2178 from the TRY database (Kattge et al., 2011), 124 samples from the Nutrient Network experiment after excluding fertilized and fenced plots (Firn et al., 2019), and 415 samples from Perkowski & Smith (2024) (see the 'Data filtering and analysis' in the Materials and Methods section). In cases where the dataset did not directly provide the year of measurement, we relied on bibliographic information within the compilations to determine the year of isotopic measurement. For each dataset, when multiple leaf δ¹³C values were available for the same species in the same year at the same site (identical longitude and latitude), we calculated the species' average isotopic values for each year at each site in each year.

Mycorrhizal association types for each genus were determined according to Soudzilovskaia et al. (2020). This classification is based on the plant genus and resulted in six plant genera groups: (1) plant genera obligatorily associated with AMF, (2) plant genera facultatively associated with AMF (capable of either AMF association or being NM), (3) plant genera associated with EcMF, (4) plant genera with dual symbiotic associations (e.g. both AMF and EcMF, observed in certain genera like poplars and eucalypts), (5) plant genera associated with ErMF, and (6) NM plant genera. We categorized plant genera associated with EcMF, ErMF, and those with dual symbiotic associations under the mining strategy. Plant genera associated with AMF or

facultatively associated with AMF were grouped under the scavenging strategy. NM plants were excluded from the dataset (see the 'Data filtering and analysis' in the Materials and Methods section).

The assignment of the ability to form symbiosis with N_2-fixing bacteria was determined by matching our dataset with the classification provided by Tedersoo et al. (2018) based on plant genus, akin to our approach for categorizing mycorrhizal symbioses.

We exclusively chose isotopic measurements from leaves of C_3 plants, including both woody and nonwoody species. Some datasets presented isotopic data in terms of carbon isotope fractionation in leaves ($\Delta^{13}C_{leaf}$) representing the difference between the isotopic composition of the atmosphere ($\delta^{13}C_{air}$) and plants ($\delta^{13}C_{leaf}$) (Farquhar et al., 1989; Feng, 1999). If only $\delta^{13}C_{leaf}$ were provided, $\Delta^{13}C_{leaf}$ value was estimated as follows:

$$\Delta^{13}C_{leaf} = \frac{\left(\delta^{13}C_{air} - \delta^{13}C_{leaf}\right)}{\left(1 + \frac{\delta^{13}C_{leaf}}{1000}\right)} \qquad \text{Eqn 1}$$

where $\delta^{13}C_{air}$ annual values were extracted from the Mauna Loa Observatory, National Oceanic and Atmospheric Administration (NOAA), based on the year of sampling (https://gml.noaa.gov/dv/data/) (Graven et al., 2017).

Climate data

Using latitude and longitude coordinates for each site, climatic data were obtained from the Climatic Research Unit at a 0.5° resolution (CRU TS3.24.01) (Harris et al., 2014). The considered climatic variables encompassed the mean annual growing season temperature (T_g; °C), atmospheric vapor pressure deficit (D_g; Pa), and mean annual precipitation (mm). Monthly and annual averages for all climate variables were computed over the period 1901–2015. The growing season was operationally defined as the months with mean temperatures exceeding 0°C. The elevation (z; m) of each site, with a resolution of 0.5°, was acquired from the WATCH Forcing Data methodology applied to ERA-Interim reanalysis meteorological forcing dataset (Weedon et al., 2014).

To assess the moisture at each site, we extracted the moisture index (hereafter MI) for the period 1970–2000 at a spatial resolution of 30 arcminutes from a global aridity database (Global-AI_PET_v3 (Zomer et al., 2022)). The MI represents the ratio of mean annual precipitation to mean annual potential evapotranspiration, accounting for both precipitation inputs and soil water loss due to the factors such as temperature, solar radiation, and wind. A lower MI indicates a more arid site.

Monthly measured atmospheric CO_2 concentrations for the 1958–2021 period were obtained from the Mauna Launa Observatory, NOAA (gml.noaa.gov/webdata/ccgg/trends/co2/co2_mm_mlo.txt; Thoning et al., 1989; Etheridge et al., 1996a,b; Keeling, 1998). These monthly measurements were averaged for each year to calculate mean annual values. For the period preceding 1958, yearly estimated CO_2 concentrations from ice cores

were obtained from the Vostok Ice Core, NASA Goddard Institute for Space Studies (data.giss.nasa.gov/modelforce/ghgases/Fig1A.ext.txt; Etheridge *et al.*, 1996a,b). Atmospheric CO_2 concentration (C_a) values were then converted from molar ratio (μmol mol^{-1}) to pressure (P_a) units using site elevation and equations described in Stocker *et al.* (2020).

Estimation of $\chi_{isotopes}$ and predictions of β via the least-cost hypothesis

We estimated $\chi_{isotopes}$ from the compiled leaf isotope fractionation ($\Delta^{13}C_{leaf}$) relative to air according to Lavergne *et al.* (2020) as:

$$\chi_{isotopes} = \frac{\left(\Delta^{13}C_{leaf} - a + f\,\frac{\Gamma^*}{C_a}\right)}{(b-a)} \qquad \text{Eqn 2}$$

where a is the fractionation associated with CO_2 diffusion (4.4‰), b is the photosynthetic fractionation by RuBisCO in C_3 plants (28‰), and f represents the isotope fractionation due to photorespiration (12‰) (Ubierna Lopez & Farquhar, 2014).

The least-cost optimality hypothesis postulates that leaves seek to minimize the cumulative unit costs of transpiration and carboxylation and provides a simple equation that defines the optimal ratio of χ to β as follows:

$$\chi = \frac{\Gamma^*}{C_a} + \left(1 - \frac{\Gamma^*}{C_a}\right)\frac{\xi}{\xi + \sqrt{D_g}} \qquad \text{Eqn 3}$$

where

$$\xi = \sqrt{\beta\,\frac{K + \Gamma^*}{1.6\eta^*}} \qquad \text{Eqn 4}$$

where the term ξ defines the sensitivity of χ to D_g (Medlyn *et al.*, 2011; Prentice *et al.*, 2014).

By substituting Eqn 4 into Eqn 3 in the model, and by replacing χ with the calculated $\chi_{isotopes}$, we derived the values of β as:

$$\beta = 1.6\,\eta^*\,D_g\,\frac{\left(\chi_{isotopes} - \frac{\Gamma^*}{C_a}\right)^2}{\left(1 - \chi_{isotopes}\right)^2 (K + \Gamma^*)} \qquad \text{Eqn 5}$$

where η^* is the viscosity of water relative to its value at 25°C, calculated using temperature and elevation as in Huber *et al.* (2009). Γ^* (P_a) is the CO_2 compensation point in the absence of mitochondrial respiration. Γ^* is temperature-dependent and was calculated following Bernacchi *et al.* (2001) using T_g and the atmospheric pressure (P_{atm}; P_a) calculated from elevation (Notes S1). C_a is the partial pressure of ambient CO_2 (P_a). K is the effective Michaelis Constant for RuBisCO-limited photosynthesis at a given partial pressure of O_2 (pO_2; P_a). K was calculated following Bernacchi *et al.* (2001) as:

$$K = K_c\left(1 + \frac{pO_2}{K_o}\right) \qquad \text{Eqn 6}$$

where K_c (P_a) and K_o (P_a) are Michaelis–Menten coefficients of RuBisCO activity for CO_2 and O_2, respectively, which are temperature-dependent (Notes S1). Further calculation details are provided in the Supporting Information.

Soil data

To estimate the soil nutrient characteristics at each site, we retrieved data on concentrations of total soil nitrogen, total soil organic carbon (SOC), and total plant-available soluble inorganic P_i. The total SOC (g C kg^{-1} soil) and total soil nitrogen (TN, g N kg^{-1} soil) were obtained from SoilGrids250m 2.0 (Poggio *et al.*, 2021) provided by the World Soil Information Service of the International Soil Reference and Information Centre (see Notes S2). For each site, we computed the average SOC and TN for the top two provided layers (0–5 cm and 5–15 cm). Subsequently, we calculated the ratio of TN to SOC at each site (soil N : C ratios, g N g^{-1} C). Instead of selecting TN as a metric for soil nitrogen status, we chose the soil N : C ratio, which reflects the soil's nitrogen-supplying potential and the balance between nitrogen and organic material. A high N : C ratio was assumed to indicate high nitrogen availability to plants.

Data on plant-available P_i concentrations (mg P kg^{-1} soil) in the top 15-cm soil layer were sourced from the global database published by McDowell *et al.* (2023). The plant-available soil P_i concentrations in this database correspond to bicarbonate-extractable Olsen P (Olsen, 1954). This database comprised 32941 geo-referenced values of Olsen P, covering 89 countries. We used the latitude and longitude coordinates of each site in our dataset to extract the corresponding plant-available P_i values. All variables used in this study are summarized in Table 2.

Data filtering and analysis

We excluded isotope-driven $\chi_{isotopes}$ values greater than 0.95 and less than 0.1, considering them as extreme values arising from uncertain parameters. The derived β values showed a departure from a normal distribution ($P < 0.001$; Shapiro–Wilk test) and exhibited skewness toward lower values. To address this, we applied a natural-log transformation to the β values to achieve a normal distribution before analysis. Outliers in the natural-log-transformed β values were removed using the median absolute deviation method, following the procedure outlined by Leys *et al.* (2013). We excluded β values deviating three times higher or lower than the median absolute deviation. Similarly, we natural-log-transformed plant-available P_i concentrations and soil N : C ratios, and we square-root-transformed the MI to meet the normality criteria for model fitting. Since the NM group represented only 2.5% of the dataset, resulting in a very small sample size compared with the mining and scavenging groups, we decided to exclude this group to avoid introducing statistical bias due to the large difference in sample sizes. Following this filtering process, we obtained a total of 4745 records for 2599 species belonging to

Table 2 Description of key abbreviated terms.

Variable	Units	Description
β	Unitless	Ratio of cost factors for carboxylation and transpiration
χ	$Pa\,Pa^{-1}$	Ratio of intercellular to extracellular CO_2 partial pressure
$\chi_{isotopes}$	$Pa\,Pa^{-1}$	Ratio of intercellular to extracellular CO_2 partial pressure calculated from leaf carbon isotopes
C_a	Pa	Partial pressure of atmospheric CO_2
C_i	Pa	Partial pressure of leaf internal CO_2
$\delta^{13}C_{leaf}$	‰	Ratio of leaf stable isotopes $^{13}C : {}^{12}C$
$\delta^{13}C_{air}$	‰	Isotopic composition of the CO_2 in atmosphere
$\Delta^{13}C_{leaf}$	‰	Carbon isotope fractionation in leaves
Γ^*	Pa	CO_2 compensation point in the absence of mitochondrial respiration
D_g	Pa	Atmospheric water vapor deficit
T_g	°C	Mean annual growing season temperature
K	Pa	Effective Michaelis constant for RuBisCO-limited photosynthesis at a given partial pressure of O_2
η^*	$Pa\,s^{-1}$	Viscosity of water relative to its value at 25°C
MI	Unitless	Moisture Index
P_i	$mg\,kg^{-1}_{soil}$	Plant-available soil phosphorus concentrations (Olsen phosphorus)
N : C	$g\,N\,g^{-1}\,C$	The ratio of soil total nitrogen to soil organic carbon concentrations

1115 genera, covering a broad range of biomes (Figs S1, S2). Plant species associated with the scavenging strategy constituted 76% of the dataset, while those with the mining strategy accounted for 24%. The N_2FP species made up 8.6% of the dataset and can belong to either the scavenging or mining strategy, with 5.8% in the mining strategy and 9.5% in the scavenging strategy.

To assess the variability of β with soil nutrients and moisture, and to examine the potential influence of mycorrhizal fungi and N_2-fixing bacteria symbioses on the relationship between β, nutrient availability, and moisture (Hypotheses 1, 2, and 3), we employed a linear mixed-effects model. The dependent variable was natural-log-transformed β, and the fixed effects included the soil natural-log-transformed N : C ratios (continuous), the natural-log-transformed plant-available P_i (continuous), the square-root-transformed MI (continuous), mycorrhizal nutrient acquisition strategy (referred to hereafter as Myco-NAS; categorical; two levels: scavenging and mining strategies), and the N_2-fixation capacity (categorical; two levels: N_2FP and OP). Given the influence of Myco-NAS on N, P, and water uptake, we included its interactions with the soil N : C ratios, plant-available P_i, and MI. For the N_2-fixation capacity, which primarily influences N uptake, we included its interaction with the soil N : C. Plant genus was included as a random intercept term. To evaluate the potential effect of multicollinearity between predictors on the interpretation of the results, we calculated variance inflation factors (VIFs) for each independent fixed effect (Davis *et al.*, 1986). We considered multicollinearity to be a concern when VIF values were above 10 (Montgomery *et al.*, 1992). Four VIF values were found to exceed the threshold of 10, specifically for N_2-fixation capacity, soil N : C ratios, and their interaction (Table 3). To address this, we removed the interaction term, as it was not significant. After this adjustment, the VIF values for all other predictors dropped below the critical threshold of 10 (Table S1). Notably, this change did not affect the outcomes or the directionality of the predictors' effects on β, suggesting that including or excluding the interaction term had no significant impact on the

results of our linear mixed-effects model. Considering this finding, the careful evaluation we performed, and the robustness of mixed-effects models even when some distributional assumptions and collinearity are violated (Schielzeth *et al.*, 2020), we decided to retain the model with the interaction term, as its exclusion did not alter the model's outcomes.

To test Hypothesis 4, and to account for the direct effects of moisture on soil N : C and plant-available P_i, while distinguishing between the direct and indirect effects of soil N : C and plant-available P_i on β via their covariance with moisture, and to assess some multicollinearities found for some predictors in the linear mixed-effects model as explained previously, we used structural equation modeling (SEM) (Fig. S3). We defined tropical and subtropical biomes to encompass the region between 30° north and south latitudes, while temperate and boreal biomes were combined for latitudes greater than 30° north and 30° south. The model was constructed with MI predicting plant-available P_i and soil N : C, while β served as the dependent variable, predicted by soil N : C, plant-available P_i, MI, Myco-NAS, and N_2-fixation capacity. Plant genus was included as a random intercept term in each model component. We performed this path analysis separately for temperate and boreal biomes, and for tropical and subtropical biomes.

The linear mixed-effects model was fit using the LMER package (Bates, 2018) in R v.4.3.2 (R Core Team, 2024). We used Type II Wald's χ^2 tests to test the statistical significance of each fixed effect term in the models using the CAR package (Fox & Weisberg, 2019) in R. *Post hoc* analyses were conducted using the 'emmeans' package (Lenth *et al.*, 2024) in R. The SEM was fit using the 'PiecewiseSEM' package (Lefcheck, 2016) using functions from the LME package (Bates, 2018) in R.

Results

Below we present data on β, with corresponding trends in $\Delta^{13}C_{leaf}$ and correlations between β and $\chi_{isotopes}$ provided in Figs S4, S5.

Table 3 Regression coefficients for the linear mixed-effects model with the carbon costs of nutrient acquisition relative to water acquisition (β) as the dependent variable.*

	df	Slope	P	VIF
Soil N : C	1	-0.41 ± 0.07	< 0.001	18
MI	1	0.06 ± 0.05	< 0.05	6
Soil Pi	1	0.03 ± 0.01	< 0.001	5
Myco-NAS	1	–	0.40	8
N_2_fixation	1	–	0.13	18
Soil N : C × Myco-NAS	1	–	< 0.05	10
MI × Myco-NAS	1	–	< 0.05	7
Soil P_i × Myco-NAS	1	–	0.3	5
Soil N : C-N_2-fixation	1	–	0.11	32

Fixed effects include plant-available soil soluble inorganic phosphorus concentration (Soil P_i), the soil nitrogen-to-organic carbon concentration ratios (Soil N : C), the moisture index (MI), mycorrhizal nutrient acquisition strategy (Myco-NAS), N_2-fixation capacity, and interactions between Myco-NAS and Soil P_i, Soil N : C and MI, as well as between N_2-fixation capacity and the soil N : C ratios.
*P-values < 0.001 are italicized. P-values < 0.05 are bolded. The sample size was 4745. No. of species = 2599. Key: Soil N : C, soil nitrogen-to-organic carbon concentration ratios (continuous); Soil P_i, plant-available soil soluble inorganic phosphorus concentration or Olsen phosphorus (continuous); MI, the moisture index (continuous); Myco-NAS, mycorrhizal nutrient acquisition strategy (categorical; mining or scavenging); N_2-fixation, ability of plant species to form symbiotic associations with N_2-fixing bacteria (categorical; N_2FP or OP). Slopes are only included for continuous fixed effects. The variance inflation factor of each variable represents the VIF. The full model conditional R^2 was 0.41.

Effects of Myco-NASs and N_2-fixation capacity on β variability in relation to soil N : C

In line with our expectations, β decreased with increasing soil N : C ratios ($P < 0.001$; Table 3). Supporting Hypothesis 1, there were significant interactions between Myco-NAS and soil N : C ratios ($P < 0.05$; Table 3). The β decrease with increasing soil N : C was more pronounced in the scavenging strategy than in the mining strategy, as confirmed by Tukey's *post hoc* test (difference between slopes: $P < 0.05$; Table 4; Fig. 3a), with both slopes being significantly negative ($P < 0.001$ in both cases; Table 4). Under low soil N : C, the mining acquisition strategy exhibited reduced β compared with the scavenging strategy, confirming Hypothesis 1 (Fig. 3a). Conversely, under higher soil N : C, the scavenging strategy had reduced β compared with the mining strategy (Fig. 3a).

Both N_2FP and OP exhibited a significant decrease in β with increasing soil N : C ratios, with each slope being significantly different from zero ($P < 0.05$; Table 3; Fig. 3b). However, contrary to our expectations (Hypothesis 2), no significant interaction between N_2-fixation capacity and soil N : C ratios was found ($P = 0.11$; Table 3), likely due to the smaller sample size of N_2FP ($n = 419$) compared with OP ($n = 4326$), and the slope for N_2FP was not significantly different from that of OP ($P = 0.15$; Table 4).

Effects of Myco-NAS on β variability in relation to the MI and P_i

Consistent with Hypothesis 3, β was positively associated with the MI ($P < 0.05$; Table 3), and there were significant interactions between the Myco-NAS and the MI ($P < 0.05$; Table 3), with a significant increase in β with increasing moisture observed only for plant species associated with the scavenging strategy ($P < 0.001$; Table 4; Fig. 4a). There was no significant relationship between β

Table 4 *Post hoc* analyses comparing the slopes of the correlations between the carbon costs of nutrient acquisition relative to water acquisition (β) and soil nitrogen-to-carbon (N : C) ratios, plant-available soil soluble inorganic phosphorus concentration (Soil P_i), and moisture index (MI) depending on mycorrhizal nutrient acquisition strategy (mining vs scavenging, for Soil P_i, Soil N : C, and MI), and on N_2-fixation (for soil N : C only).*

	Slope	P-values
Soil N : C – mining strategy	-0.32 ± 0.09^a	< 0.001
Soil N : C – scavenging strategy	-0.50 ± 0.07^b	< 0.001
Soil P_i – mining strategy	0.02 ± 0.026^a	0.44
Soil P_i – scavenging strategy	0.05 ± 0.01^a	< 0.001
MI – mining strategy	-0.06 ± 0.1^a	0.55
MI – scavenging strategy	0.18 ± 0.05^b	< 0.001
Soil N : C – N_2FP	-0.52 ± 0.13^a	< 0.001
Soil N : C – OP	-0.31 ± 0.04^a	< 0.001

*P-values < 0.001 are italicized. The sample size was 4745. No. of species = 2599. Key: Soil N : C, soil nitrogen-to-organic carbon concentration ratios (continuous); Soil P_i, plant-available soil soluble inorganic phosphorus concentration or Olsen phosphorus (continuous); MI, the moisture index (continuous), mycorrhizal nutrient acquisition strategy (categorical; mining or scavenging), ability of plant species to form symbiotic association with N_2-fixing bacteria (categorical; N_2FP or OP). Slopes for each category are presented. When P-values are < 0.05, we consider the slopes to differ significantly from zero. Superscript letters represent comparisons between slopes using the Tukey test within each mycorrhizal category with respect to Soil P_i, Soil N : C ratios, and MI, and within each N_2-fixation category with respect to the Soil N : C ratios. For each fixed effect (Soil P_i, Soil N : C ratios, and MI), slopes that do not share a letter are significantly different according to the Tukey test at the 5% significance level.

and the MI for plant species associated with the mining strategy ($P = 0.55$; Table 4; Fig. 4a). Unexpectedly, β increased significantly with increasing plant-available P_i ($P < 0.001$; Table 3; Fig. 4b). However, we did not find any significant interaction between Myco-NAS and plant-available P_i ($P = 0.3$; Table 3).
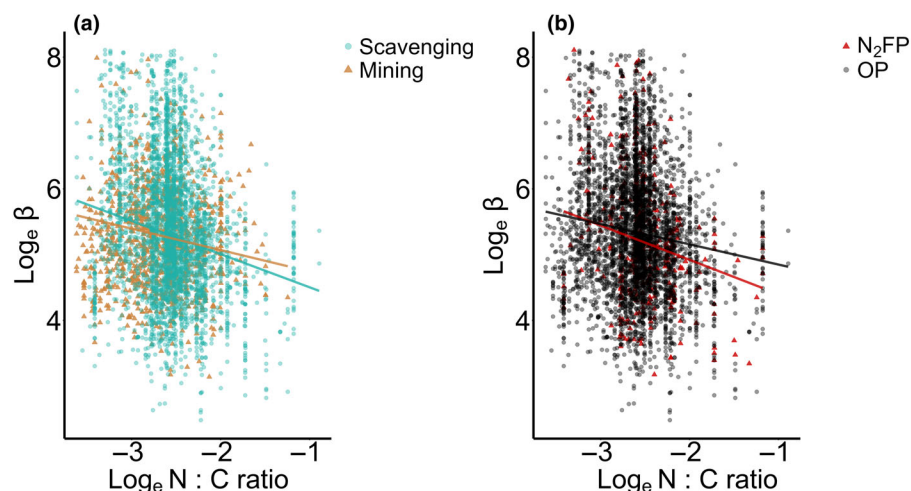
Fig. 3 Fitted linear regression plots illustrating the correlations between natural-log-transformed carbon costs of nutrient acquisition relative to water acquisition (β) and natural-log-transformed soil nitrogen-to-carbon (N : C) ratios for (a) each mycorrhizal nutrient acquisition strategy (Myco-NAS) and (b) N_2-fixation capacity. The regressions are derived from the linear mixed-effects models explained in Tables 3 and 4. Individual data points are represented by dots and triangles: light green dots (scavenging strategy), light orange triangles (mining strategy), black dots (other plants), and red dots (N_2-fixing plants). Separate lines are plotted for each Myco-NAS and N_2-fixation capacity, with colors corresponding to the respective strategy. Solid lines indicate statistically significant trends ($P < 0.05$).
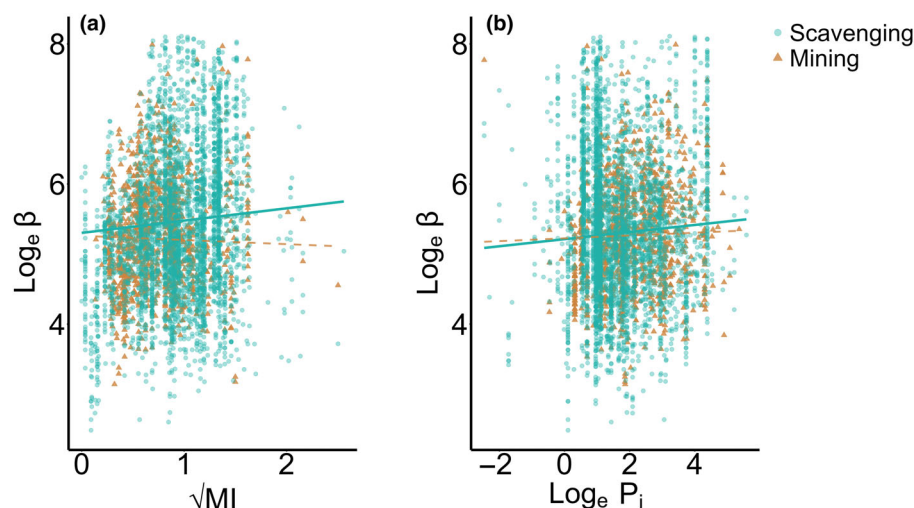

Fig. 4 Fitted linear regression plots illustrating the correlations between (a) natural-log-transformed carbon costs of nutrient acquisition relative to water acquisition (β) and the square root of the moisture index and (b) natural-log-transformed β and natural-log plant-available soil soluble inorganic phosphorus concentration for each mycorrhizal nutrient acquisition strategy (Myco-NAS). The regressions are derived from the linear mixed-effects models explained in Tables 3 and 4. Individual data points are represented by dots and triangles: light green dots (scavenging strategy), light orange triangles (mining strategy). Separate lines are plotted for each Myco-NAS, with colors corresponding to the respective strategy. Solid lines indicate statistically significant trends ($P < 0.05$), while dashed lines represent nonsignificant trends ($P > 0.05$).

Factors controlling β variability depending on N and P colimitation

The path analysis aimed to disentangle the direct effects of soil N : C and plant-available soil P_i on β, as well as their indirect effects through their covariance with the MI, considering biomes and the hypothesized N and P limitations in each biome. Before presenting the path analysis results, we explored

the differences in soil N : C ratios and soil P_i concentration between biomes (Fig. S6). As expected, tropical and subtropical biomes exhibited significantly lower P_i concentrations and, to a lesser extent, lower soil N : C ratios than temperate and boreal biomes, suggesting that tropical and subtropical biomes are colimited by N and P. The path analysis for temperate and boreal biomes revealed that soil N : C ratios were the only factor negatively affecting β (standardized estimate

Tropical and subtropical biomes **(a)**
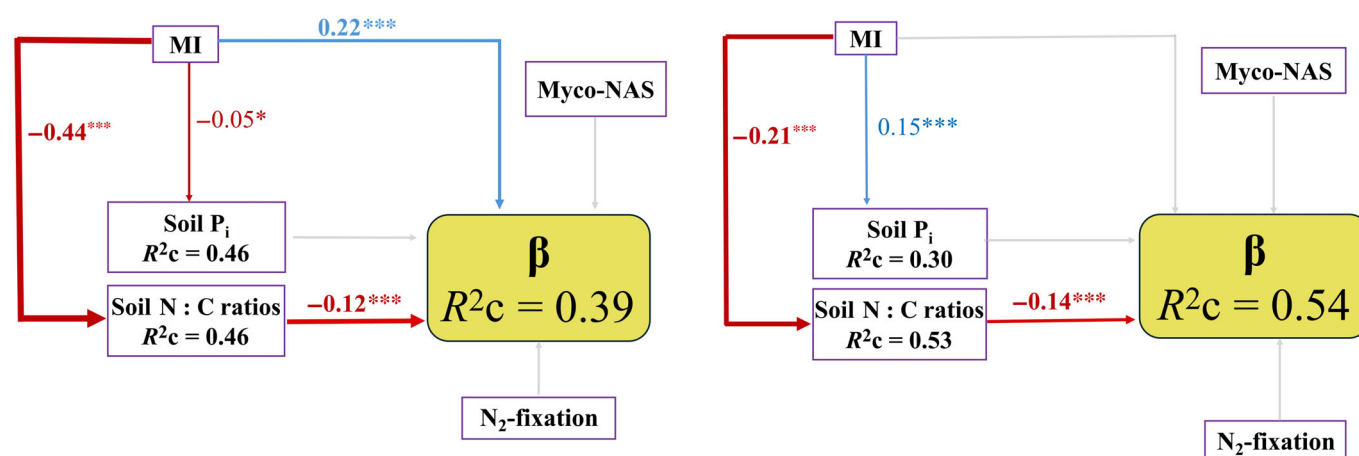
Temperate and boreal biomes **(b)**

Fig. 5 Structural equation model showing the direct effects of the moisture index (MI) on soil soluble plant-available phosphorus (Soil P_i) concentrations and the soil nitrogen-to-carbon (N : C) ratios, as well as the effects of MI, Soil P_i, Soil N : C ratios, mycorrhizal association types (Myco-NAS), and N_2-fixation on the carbon costs of nutrient acquisition relative to water acquisition (β) in (a) tropical and subtropical biomes ($n = 2264$, 268 mining strategy, 1996 scavenging strategy), and (b) temperate and boreal biomes ($n = 2481$, 872 mining strategy, 1609 scavenging strategy). Arrows represent unidirectional correlations between variables. Path coefficients are depicted as simple standardized regression coefficients. Stars in subscripts represent the significance levels (***, $P < 0.001$; *, $P < 0.05$). The width of connections indicates estimates of standardized path coefficients, with solid lines denoting significant connections and semitransparent gray lines indicating nonsignificant connections that were included in the model. Red arrows denote negative correlations, and blue arrows positive ones. The coefficients of determination are reported as conditional R^2_c, which is based on the variance of both the fixed and random effects.

coefficient $= -0.14$; Fig. 5b). The MI decreased soil N : C ratios (standardized estimate coefficient $= -0.21$; Fig. 5b) and increased plant-available P_i (standardized estimate coefficient $= 0.15$; Fig. 5b), but neither P_i nor the MI directly affected β in these biomes. By contrast, the path analysis for tropical and subtropical biomes showed that β was significantly positively affected by MI (standardized estimate coefficient $= 0.22$; Fig. 5a) and negatively affected by soil N : C (standardized estimate coefficient $= -0.12$; Fig. 5a), with no significant effect of P_i. Both P_i and soil N : C significantly decreased with increasing MI (standardized estimate coefficients $= -0.05$ and -0.44, respectively; Fig. 5a). These results clarify the observed increase in β with P_i identified by the linear mixed-effects model, which does not account for the indirect effects of MI on P_i depending on the biome. The path analysis demonstrates that in tropical and subtropical biomes, MI reduces P_i directly, thereby nullifying P_i's influence on β.

Discussion

A significant source of uncertainty in the projections of future ecosystem carbon budget by ESMs resides in their formulation of photosynthetic acclimation to soil resources and climate, as well as the carbon costs of acquiring resources (Booth *et al.*, 2012; Smith, 2024). The photosynthetic least-cost hypothesis provides a possible way to reliably simulate these responses (Prentice *et al.*, 2014; Wang *et al.*, 2017a,b; Smith *et al.*, 2019; Paillassa *et al.*, 2020; Stocker *et al.*, 2020), but data are needed to evaluate

the theory at scales relevant for ESMs (i.e. local to global). We addressed this challenge by analyzing a key variable in the quantified least-cost hypothesis (Prentice *et al.*, 2014), namely, the carbon costs of nutrient acquisition relative to water acquisition (β), which has been historically held constant in EEO models that adopt photosynthetic least-cost principles (Wang *et al.*, 2017b; Stocker *et al.*, 2020). Using a global dataset of leaf carbon isotopes to estimate these costs, our findings revealed significant, complex, yet predictable variability in the costs of acquiring soil resources, as modulated by soil nutrient availability, moisture, and plant nutrient acquisition strategy.

Nutrient acquisition strategies modulate β variability in relation to soil N : C ratios

Across biomes and nutrient acquisition strategies, a consistent pattern emerges: The carbon costs of nutrient acquisition relative to water acquisition decreased with increasing soil N : C ratios. This supports the efficacy of least-cost principles in predicting the reduced carbon costs for nutrient acquisition when N is abundant and readily available in the soil. These findings emphasize the critical role of soil N in driving the observed variability in carbon costs at a global scale and validate the formulation of resource uptake models predicting reduced carbon costs of acquiring N with increasing N availability across both mycorrhizal and NM strategies (Meyer *et al.*, 2010; Phillips *et al.*, 2013; Brzostek *et al.*, 2014; Braghiere *et al.*, 2021, 2022; Wang *et al.*, 2022).

We found significant interactions between the soil N : C ratios and the Myco-NAS in modulating β (Fig. 5a). While experimental evidence (Wallander & Nylund, 1992; Gorissen et al., 1993; Olsson et al., 2005; Hasselquist et al., 2012; Kjøller et al., 2012; Högberg et al., 2021; R. Wang et al., 2021) and meta-analyses (Treseder, 2004; Gill & Finzi, 2016; Han et al., 2020) have demonstrated reduced carbon allocation to mycorrhizal fungi with increasing soil N availability, our findings highlight that this response is influenced by the mycorrhizal functional group. This may suggest that plants optimize carbon allocation to minimize nutrient acquisition costs, emphasizing the importance of incorporating this modulation into ESMs.

At low soil N : C ratios, the mining strategy (e.g. association with EEMF) demonstrated reduced β compared with the scavenging strategy (e.g. association with AMF). Conversely, under high soil N : C ratios, the scavenging strategy showed reduced β compared with the mining strategy. These findings align with the proposed framework of distinct nutrient economies associated with mycorrhizal types (Read, 1991; Phillips et al., 2013). EEMF-associated plants, primarily woody species found in temperate and boreal forests, produce recalcitrant litter characterized by low N : C ratios and slow decomposition (Read, 1991; Phillips et al., 2013). This reduces N mineralization and availability in soils (Cornelissen et al., 2007), promotes an organic-nutrient economy, and enables EEMF mycelium to extract N from organic pools. Indeed, the EEMF strategy is most abundant in these 'slow' nitrogen cycling ecosystems (Pritsch & Garbaye, 2011; Rineau & Courty, 2011; Wolfe et al., 2012; Frey, 2019). By contrast, AMF-associated plants, including herbaceous and woody species, produce litter with high N : C ratios with rapid mineralization. This enriches soils with soluble N (Read, 1991; Smith & Read, 2010; Phillips et al., 2013; Jo et al., 2019), supports an inorganic-nutrient economy (Cheng et al., 2012; Mei et al., 2022), and enables AMF to efficiently scavenge N. The AMF strategy is most abundant in these 'fast' nitrogen cycling ecosystems (Read, 1991; Read & Perez-Moreno, 2003; Phillips et al., 2013). This can also explain the nutrient-acquisitive trait profile in AMF-associated plants and the nutrient-conservative trait profile in EEMF-associated plants (Averill et al., 2019).

In fact, the observed shift toward AMF tree dominance in regions with elevated atmospheric nitrogen deposition (Averill et al., 2018; Crowther et al., 2019; Lilleskov et al., 2019; Braghiere et al., 2021) supports this framework. Evidence suggests AMF-associated plants may have limited N uptake when soil N is low (Reynolds et al., 2005; Bücking & Kafle, 2015; Bowles et al., 2018), but thrive in nitrogen-rich environments compared with EcMF-associated plants (McNeil et al., 2007; Thomas et al., 2015). While AMF-associated trees have demonstrated positive net primary production responses to soil N enrichment (McNeil et al., 2007), EcMF-associated trees have exhibited more variable responses (i.e., some increased their NPP, some decreased, and some were unaffected; Thomas et al., 2015), indicating the uncertain benefits of EcMF in nitrogen-rich environments. However, EcMF symbiosis has been shown to be beneficial in nitrogen-impoverished environments for N acquisition (Lindahl & Tunlid, 2015; Shah et al., 2016). For instance, meta-analyses have demonstrated that under elevated CO_2, EcMF enhanced plant NPP and reduced carbon costs for nitrogen acquisition compared with AMF (Terrer et al., 2016, 2018; Liu et al., 2024). This suggests that under elevated CO_2, the presumed higher plant N requirement leads to the depletion of the inorganic soil N pool, favoring EcMF, as some are capable of decomposing soil organic materials.

N_2-fixing plants show similar costs to other plants, regardless of soil N : C ratios

Contrary to our expectations (Fig. 2b), we found no significant interactions between N_2-fixation capacity and soil N : C ratios on β, nor did N₂FP show reduced β at low soil N : C ratios compared with OP. While many studies have shown that high soil N can decrease nodulation rates (Barron et al., 2011; Batterman et al., 2013; Sullivan et al., 2014; Perkowski et al., 2021), others have reported minimal effects of soil N levels on symbiotic N_2-fixation (Drake, 2011; Vitousek et al., 2013), suggesting comparable N acquisition costs. Our results align with the latter findings. Additionally, modeling studies have also proposed that N_2-fixation is cost-effective only under severe N limitation (Menge et al., 2009, 2015, 2017). Nonetheless, identifying the precise soil N : C ratio threshold for severe N limitation in our dataset remains challenging. It has also been proposed that facultative symbiosis is evolutionarily advantageous in environments with fluctuating soil N levels, in which adjusting the symbiosis is not costly, whereas obligate symbiosis may be more advantageous in consistently N-limited environments (e.g. tropical latitudes), in which the cost of adjusting symbiosis is high (Menge et al., 2009, 2017). Additionally, other potential mechanisms could explain the dominance of N_2-fixing species in water-limited ecosystems at low latitudes, such as plant water savings and higher leaf N content (Adams et al., 2016; Querejeta et al., 2022). Future studies should examine the differences between facultative and obligate symbiotic N_2-fixation in relation to soil N under different water availability contexts.

Moisture shapes β differently depending on nutrient acquisition strategies

We observed that β increased with MI as expected in AMF-associated plants (scavenging strategy), but, unexpectedly, not in EEMF-associated plants (mining strategy). Under dry conditions, low β values may result from increased carbon costs associated with maintaining transpiration ($a_β$). Optimality partitioning theory and experimental evidence, especially from tree species seedlings, suggest that the root:shoot ratio increases with increasing aridity (Poorter et al., 2012; Ledo et al., 2018). Additionally, plants might allocate more carbon belowground to their fungal partners to alleviate drought stress. The opposite is expected when moisture increases. Both AMF and EEMF have been reported to play crucial roles in water uptake by forming hyphal avenues for water and nutrients in arid soils (Duddridge et al., 1980; Agerer, 2001; Egerton-Warburton et al., 2003;

Querejeta *et al.*, 2003, 2006; Bornyasz *et al.*, 2005; Allen, 2007; Lehto & Zwiazek, 2011; Ruth *et al.*, 2011; Augé *et al.*, 2015; Castaño *et al.*, 2023). However, AMF-associated plants are more common in dry, hot environments (Jo *et al.*, 2019), so β may be strongly reduced by aridity in these plants compared with EEMF-associated plants. For instance, AMF symbiosis has been reported to benefit drought-stressed plants and increase water use efficiency (Ruiz-Lozano *et al.*, 1995; Querejeta *et al.*, 2006; Nouri *et al.*, 2020; Madouh & Quoreshi, 2023) by enhancing stomatal conductance, which increases transpiration and photosynthesis (Augé, 2001; Augé *et al.*, 2015, 2016). AMF-associated plants are also favored over EcMF-associated ones in water-limited systems due to their greater hyphal plasticity and ability to function under negative water potentials (Querejeta *et al.*, 2009; Tedersoo & Brundrett, 2017; Jo *et al.*, 2019), with higher AMF hyphal abundance observed in dry soils (Hawkes *et al.*, 2011). However, it has also been reported that not all AMF species or isolates of a species have the same water uptake capacity or resistance to drought, as these factors depend on the intensity and duration of water stress and the carbon supply from the host plant (Zhang *et al.*, 2018; Leyva-Morales *et al.*, 2019).

At the same time, soluble nutrient uptake, primarily through direct root uptake, is sensitive to water availability (Barber, 1995; Leadley *et al.*, 1997; McMurtrie & Näsholm, 2018). Reduced transpiration under dry conditions limits soluble nutrient uptake via mass flow and diffusion (Nye, 1977; Gerber *et al.*, 2010; Oyewole *et al.*, 2014; Salazar-Tortosa *et al.*, 2018; Joseph *et al.*, 2021), and drought has been reported to reduce plant N and P due to water limitation rather than nutrient scarcity (He & Dijkstra, 2014). Some studies have reported that when plants are unable to access N through interception or diffusion, they increase their stomatal conductance and transpiration as a strategy to acquire N via mass flow (Cramer *et al.*, 2008; Matimati *et al.*, 2014). As a result, increasing aridity should increase both the carbon costs for water and nutrient uptake. We found that aridity decreased the carbon costs of nutrient acquisition relative to water acquisition (β), suggesting that moisture had a greater impact on water costs than nutrient costs for AMF-associated plants. By contrast, EEMF-associated plants showed no change in β with changing moisture. If we assume that water acquisition costs decrease with increasing moisture for EEMF-associated plants, then our results would suggest that moisture has a similar relative impact on nutrient acquisition costs in these plants. This may be due to the fact that moisture can impact EEMF-derived organic matter decomposition (Talbot *et al.*, 2008).

N-P colimitation modulates β

Our findings highlighted the role of N–P colimitation and its interaction with moisture in shaping β (Fig. 5). At temperate and boreal latitudes, where N is typically reported to be more limiting than P, our path analysis showed that carbon costs of nutrient acquisition relative to water acquisition decreased only with increasing soil N : C ratios. There was no direct effect of P_i or MI on these costs. This suggests that in regions where P and N are primarily present in organic, insoluble complexes and N is the

main limiting factor, carbon costs are influenced by soil N : C ratios rather than the availability of soluble P_i.

Conversely, at tropical and subtropical latitudes, where N and P are reported to colimit plant growth (Vitousek, 2004; Vitousek *et al.*, 2010; Laliberté *et al.*, 2015; Camenzind *et al.*, 2018), the carbon costs of nutrient acquisition relative to water acquisition decreased with increasing soil N : C ratios and increased with higher moisture levels, as expected. However, no direct effects of P_i availability on β were observed. This result can only be understood in the context of the interaction between MI and plant-available Pi. When the direct effects of moisture on soil Pi were accounted for, our path analysis revealed that the absence of Pi's direct effects on β was due to these effects being mediated through moisture. Specifically, the negative correlation between MI and soil Pi availability we observed aligns with previous findings in drylands, where soil Pi concentrations increased with aridity (Delgado-Baquerizo *et al.*, 2013, 2018). While our tropical and subtropical sites were not exclusively drylands, 36% were classified as dry sites and 64% were humid sites.

Carbon as a cost or just a surplus?

Finally, one could rightly argue that our approach is biased for assuming that carbon allocated to belowground resource acquisition is a major cost to plants. Indeed, some studies have suggested carbon transfer to symbionts occurs independently of nutrient exchange (Corrêa *et al.*, 2012; Prescott *et al.*, 2020). Our approach has been criticized for framing carbon as the sole fitness metric, reducing plant fitness costs to a single currency (i.e. carbon), and aligning this with economic concepts such as 'optimization' and 'trade-offs' (Prescott *et al.*, 2020; Blonder *et al.*, 2023; Roddy, 2023; Prescott, 2024). Alternative hypotheses propose that carbon transferred to mycorrhizal fungi represents surplus due to growth limitations from nutrients, rather than a 'cost' (Prescott *et al.*, 2020; Bunn *et al.*, 2024). These perspectives, while distinct, may complement each other, offering a more integrated understanding of plant processes at the whole-plant level (for a comprehensive review of this ongoing debate, we refer readers to Bunn *et al.*, 2024). Nonetheless, the alignment of variation in observed resource–soil acquisition costs with our predictions supports that carbon is an important, nonsurplus currency for soil resource acquisition.

Limitations

This study has limitations due to data constraints. Assigning mycorrhizal types to plant genera may oversimplify symbiosis dynamics, as some species host multiple fungi and shift between AMF and EcMF, or between NM and AMF based on environmental conditions (Brundrett & Tedersoo, 2018; Teste *et al.*, 2020). Dual symbioses with N_2-fixing bacteria and AMF further complicate nutrient acquisition, with P availability affecting nodulation and N availability influencing AMF phosphatase production (Leidi & Rodríguez-Navarro, 2000; Augusto *et al.*, 2013). Additionally, since nutrient uptake in the rhizosphere is a highly localized process, limited data on soil N forms

and high-resolution measurements of plant-available Pi restrict accurate carbon cost assessments across mycorrhizal types. Future experiments at finer scales are essential to validate these global-scale patterns.

Here, we found that soil resource acquisition costs are driven by interactions between soil resource availability and acquisition strategy. Our results suggest that plants minimize these costs in a predictable way dependent on their environment and resource acquisition strategy. Our results can be used to refine and test ESMs that implement mycorrhizal-dependent carbon–nutrient–water interactions.

Competing interests

None declared.

Author contributions

AC, JC and NGS conceived the study and conducted data synthesis. AC and NGS performed data analyses. AC drafted the manuscript, and all coauthors provided input on subsequent drafts.

ORCID

Alissar Cheaib https://orcid.org/0009-0004-4481-7976
Evan A. Perkowski https://orcid.org/0000-0002-9523-8892
Nicholas G. Smith https://orcid.org/0000-0001-7048-4387

Data availability

All data and code used for these analyses are available at: doi: 10.5281/zenodo.14774016.

References

Adams MA, Turnbull TL, Sprent JI, Buchmann N. 2016. Legumes are different: Leaf nitrogen, photosynthesis, and water use efficiency. *Proceedings of the National Academy of Sciences, USA* **113**: 4098–4103.

Agerer R. 2001. Exploration types of ectomycorrhizae. *Mycorrhiza* **11**: 107–114.

Allen K, Fisher JB, Phillips RP, Powers JS, Brzostek ER. 2020. Modeling the carbon cost of plant nitrogen and phosphorus uptake across temperate and tropical forests. *Frontiers in Forests and Global Change* **3**: 43.

Allen MF. 2007. Mycorrhizal fungi: highways for water and nutrients in arid soils. *Vadose Zone Journal* **6**: 291–297.

Augé RM. 2001. Water relations, drought and vesicular-arbuscular mycorrhizal symbiosis. *Mycorrhiza* **11**: 3–42.

Augé RM, Sylvia DM, Park S, Buttery BR, Saxton AM, Moore JL, Cho K. 2004. Partitioning mycorrhizal influence on water relations of Phaseolus vulgaris into soil and plant components. *Canadian Journal of Botany* **82**: 503–514.

Augé RM, Toler HD, Saxton AM. 2015. Arbuscular mycorrhizal symbiosis alters stomatal conductance of host plants more under drought than under amply watered conditions: a meta-analysis. *Mycorrhiza* **25**: 13–24.

Augé RM, Toler HD, Saxton AM. 2016. Mycorrhizal stimulation of leaf gas exchange in relation to root colonization, shoot size, leaf phosphorus and nitrogen: a quantitative analysis of the literature using meta-regression. *Frontiers in Plant Science* **7**: 1084.

Augusto L, Delerue F, Gallet-Budynek A, Achat DL. 2013. Global assessment of limitation to symbiotic nitrogen fixation by phosphorus availability in terrestrial ecosystems using a meta-analysis approach. *Global Biogeochemical Cycles* **27**: 804–815.

Averill C, Bhatnagar JM, Dietze MC, Pearse WD, Kivlin SN. 2019. Global imprint of mycorrhizal fungi on whole-plant nutrient economics. *Proceedings of the National Academy of Sciences, USA* **116**: 23163–23168.

Averill C, Dietze MC, Bhatnagar JM. 2018. Continental-scale nitrogen pollution is shifting forest mycorrhizal associations and soil carbon stocks. *Global Change Biology* **24**: 4544–4553.

Barber SA. 1962. A diffusion and mass-flow concept of soil nutrient availability. *Soil Science* **93**: 39–49.

Barber SA. 1995. *Soil nutrient bioavailability: a mechanistic approach.* New York, NY, USA: John Wiley & Sons.

Barceló M, Van Bodegom PM, Soudzilovskaia NA. 2023. Fine-resolution global maps of root biomass carbon colonized by arbuscular and ectomycorrhizal fungi. *Scientific Data* **10**: 56.

Barron AR, Purves DW, Hedin LO. 2011. Facultative nitrogen fixation by canopy legumes in a lowland tropical forest. *Oecologia* **165**: 511–520.

Bates DM. 2018. lme4: mixed-effects modeling with R.

Batterman SA, Hedin LO, Van Breugel M, Ransijn J, Craven DJ, Hall JS. 2013. Key role of symbiotic dinitrogen fixation in tropical forest secondary succession. *Nature* **502**: 224–227.

Bending GD, Read DJ. 1997. Lignin and soluble phenolic degradation by ectomycorrhizal and ericoid mycorrhizal fungi. *Mycological Research* **101**: 1348–1354.

Bennett AE, Groten K. 2022. The costs and benefits of plant–arbuscular mycorrhizal fungal interactions. *Annual Review of Plant Biology* **73**: 649–672.

Bernacchi CJ, Singsaas EL, Pimentel C, Portis AR Jr, Long SP. 2001. Improved temperature response functions for models of Rubisco-limited photosynthesis. *Plant, Cell & Environment* **24**: 253–259.

Blonder BW, Aparecido LMT, Hultine KR, Lombardozzi D, Michaletz ST, Posch BC, Slot M, Winter K. 2023. Plant water use theory should incorporate hypotheses about extreme environments, population ecology, and community ecology. *New Phytologist* **238**: 2271–2283.

Booth BBB, Jones CD, Collins M, Totterdell IJ, Cox PM, Sitch S, Huntingford C, Betts RA, Harris GR, Lloyd J. 2012. High sensitivity of future global warming to land carbon cycle processes. *Environmental Research Letters* **7**: 024002.

Bornyasz MA, Graham RC, Allen MF. 2005. Ectomycorrhizae in a soil-weathered granitic bedrock regolith: linking matrix resources to plants. *Geoderma* **126**: 141–160.

Bowles TM, Jackson LE, Cavagnaro TR. 2018. Mycorrhizal fungi enhance plant nutrient acquisition and modulate nitrogen loss with variable water regimes. *Global Change Biology* **24**: e171–e182.

Braghiere RK, Fisher JB, Allen K, Brzostek E, Shi M, Yang X, Ricciuto DM, Fisher RA, Zhu Q, Phillips RP. 2022. Modeling global carbon costs of plant nitrogen and phosphorus acquisition. *Journal of Advances in Modeling Earth Systems* **14**: e2022MS003204.

Braghiere RK, Fisher JB, Fisher RA, Shi M, Steidinger BS, Sulman BN, Soudzilovskaia NA, Yang X, Liang J, Peay KG et al. 2021. Mycorrhizal distributions impact global patterns of carbon and nutrient cycling. *Geophysical Research Letters* **48**: e2021GL094514.

Brundrett MC. 2009. Mycorrhizal associations and other means of nutrition of vascular plants: understanding the global diversity of host plants by resolving conflicting information and developing reliable means of diagnosis. *Plant and Soil* **320**: 37–77.

Brundrett MC, Tedersoo L. 2018. Evolutionary history of mycorrhizal symbioses and global host plant diversity. *New Phytologist* **220**: 1108–1115.

Brzostek ER, Finzi AC. 2011. Substrate supply, fine roots, and temperature control proteolytic enzyme activity in temperate forest soils. *Ecology* 92: 892–902.

Brzostek ER, Fisher JB, Phillips RP. 2014. Modeling the carbon cost of plant nitrogen acquisition: mycorrhizal trade-offs and multipath resistance uptake improve predictions of retranslocation: carbon cost of mycorrhizae. *Journal of Geophysical Research: Biogeosciences* 119: 1684–1697.

Bücking H, Kafle A. 2015. Role of arbuscular mycorrhizal fungi in the nitrogen uptake of plants: current knowledge and research gaps. *Agronomy* 5: 587–612.

Bunn RA, Corrêa A, Joshi J, Kaiser C, Lekberg Y, Prescott CE, Sala A, Karst J. 2024. What determines transfer of carbon from plants to mycorrhizal fungi? *New Phytologist* 244: 1199–1215. doi: 10.1111/nph.20145.

Camenzind T, Hättenschwiler S, Treseder KK, Lehmann A, Rillig MC. 2018. Nutrient limitation of soil microbial processes in tropical forests. *Ecological Monographs* 88: 4–21.

Castaño C, Suarez-Vidal E, Zas R, Bonet JA, Oliva J, Sampedro L. 2023. Ectomycorrhizal fungi with hydrophobic mycelia and rhizomorphs dominate in young pine trees surviving experimental drought stress. *Soil Biology and Biochemistry* 178: 108932.

Chapin FS III, Autumn K, Pugnaire F. 1993. Evolution of suites of traits in response to environmental stress. *The American Naturalist* 142: S78–S92.

Chapman N, Miller AJ, Lindsey K, Whalley WR. 2012. Roots, water, and nutrient acquisition: let's get physical. *Trends in Plant Science* 17: 701–710.

Chen G, Yang Y, Robinson D. 2014. Allometric constraints on, and trade-offs in, belowground carbon allocation and their control of soil respiration across global forest ecosystems. *Global Change Biology* 20: 1674–1684.

Cheng L, Booker FL, Tu C, Burkey KO, Zhou L, Shew HD, Rufty TW, Hu S. 2012. Arbuscular mycorrhizal fungi increase organic carbon decomposition under elevated CO_2. *Science* 337: 1084–1087.

Cornelissen JHC, Van Bodegom PM, Aerts R, Callaghan TV, Van Logtestijn RSP, Alatalo J, Stuart Chapin F, Gerdol R, Gudmundsson J, Gwynn-Jones D et al. 2007. Global negative vegetation feedback to climate warming responses of leaf litter decomposition rates in cold biomes. *Ecology Letters* 10: 619–627.

Cornwell WK, Wright IJ, Turner J, Maire V, Barbour MM, Cernusak LA, Dawson T, Ellsworth D, Farquhar GD, Griffiths H et al. 2018. Climate and soils together regulate photosynthetic carbon isotope discrimination within C_3 plants worldwide. *Global Ecology and Biogeography* 27: 1056–1067.

Corrêa A, Gurevitch J, Martins-Loução MA, Cruz C. 2012. C allocation to the fungus is not a cost to the plant in ectomycorrhizae. *Oikos* 121: 449–463.

Cowan IR, Farquhar GD. 1977. Stomatal function in relation to leaf metabolism and environment. *Symposia of the Society for Experimental Biology* 31: 471–505.

Cramer MD, Hoffmann V, Verboom GA. 2008. Nutrient availability moderates transpiration in *Ehrharta calycina*. *New Phytologist* 179: 1048–1057.

Crowther TW, Liang J, Van Nuland ME, Werner GDA, Reich PB, Nabuurs G, de-Miguel S, Zhou M, Picard N, Herault B. 2019. Climatic controls of decomposition drive the global biogeography of forest-tree symbioses. *Nature* 569: 404–408.

Davis CE, Hyde JE, Bangdiwala SI, Nelson JJ. 1986. An example of dependencies among variables in a conditional logistic regression. In: *Modern statistical methods in chronic disease epidemiology*. New York, NY, USA: Wiley, 140–147.

Dekker LW, Ritsema CJ. 1996. Preferential flow paths in a water repellent clay soil with grass cover. *Water Resources Research* 32: 1239–1249.

Delgado-Baquerizo M, Eldridge DJ, Maestre FT, Ochoa V, Gozalo B, Reich PB, Singh BK. 2018. Aridity decouples C:N:P stoichiometry across multiple trophic levels in terrestrial ecosystems. *Ecosystems* 21: 459–468.

Delgado-Baquerizo M, Maestre FT, Gallardo A, Bowker MA, Wallenstein MD, Quero JL, Ochoa V, Gozalo B, García-Gómez M, Soliveres S et al. 2013. Decoupling of soil nutrient cycles as a function of aridity in global drylands. *Nature* 502: 672–676.

Diefendorf AF, Mueller KE, Wing SL, Koch PL, Freeman KH. 2010. Global patterns in leaf ^{13}C discrimination and implications for studies of past and future climate. *Proceedings of the National Academy of Sciences, USA* 107: 5738–5743.

Douds DD, Johnson CR, Koch KE. 1988. Carbon cost of the fungal symbiont relative to net leaf P accumulation in a split-root VA mycorrhizal symbiosis. *Plant Physiology* 86: 491–496.

Drake DC. 2011. Invasive legumes fix N_2 at high rates in riparian areas of an N-saturated, agricultural catchment. *Journal of Ecology* 99: 515–523.

Drigo B, Pijl AS, Duyts H, Kielak AM, Gamper HA, Houtekamer MJ, Boschker HTS, Bodelier PLE, Whiteley AS, Van Veen JA et al. 2010. Shifting carbon flow from roots into associated microbial communities in response to elevated atmospheric CO_2. *Proceedings of the National Academy of Sciences, USA* 107: 10938–10942.

Du E, Terrer C, Pellegrini AFA, Ahlström A, Van Lissa CJ, Zhao X, Xia N, Wu X, Jackson RB. 2020. Global patterns of terrestrial nitrogen and phosphorus limitation. *Nature Geoscience* 13: 221–226.

Duddridge JA, Malibari A, Read DJ. 1980. Structure and function of mycorrhizal rhizomorphs with special reference to their role in water transport. *Nature* 287: 834–836.

Egerton-Warburton LM, Graham RC, Hubbert KR. 2003. Spatial variability in mycorrhizal hyphae and nutrient and water availability in a soil-weathered bedrock profile. *Plant and Soil* 249: 331–342.

Elser JJ, Bracken MES, Cleland EE, Gruner DS, Harpole WS, Hillebrand H, Ngai JT, Seabloom EW, Shurin JB, Smith JE. 2007. Global analysis of nitrogen and phosphorus limitation of primary producers in freshwater, marine and terrestrial ecosystems. *Ecology Letters* 10: 1135–1142.

Etheridge DM, Steele LP, Langenfelds RL, Francey RJ, Barnola J-M, Morgan VI. 1996a. Natural and anthropogenic changes in atmospheric CO_2 over the last 1000 years from air in Antarctic ice and firn. *Journal of Geophysical Research: Atmospheres* 101: 4115–4128.

Farquhar GD, Buckley TN, Miller JM. 2002. Optimal stomatal control in relation to leaf area and nitrogen content. *Silva Fennica* 36: 625–637.

Farquhar GD, Ehleringer JR, Hubic KT. 1989. Carbon isotope discrimination and photosynthesis. *Annual Review of Plant Physiology and Plant Molecular Biology* 40: 503–537.

Feng X. 1999. Trends in intrinsic water-use efficiency of natural trees for the past 100–200 years: a response to atmospheric CO_2 concentration. *Geochimica et Cosmochimica Acta* 63: 1891–1903.

Field CH. 1986. The photosynthesis-nitrogen relationship in wild plants. In: *On the economy of plant form and function*, 25–55. Cambridge, UK: Cambridge University Press.

Finke RL, Harper JE, Hageman RH. 1982. Efficiency of nitrogen assimilation by N_2-Fixing and nitrate-grown soybean plants (*Glycine max* [L.] Merr.). *Plant Physiology* 70: 1178–1184.

Finzi AC, Austin AT, Cleland EE, Frey SD, Houlton BZ, Wallenstein MD. 2011. Responses and feedbacks of coupled biogeochemical cycles to climate change: examples from terrestrial ecosystems. *Frontiers in Ecology and the Environment* 9: 61–67.

Firn J, McGree JM, Harvey E, Flores-Moreno H, Schütz M, Buckley YM, Borer ET, Seabloom EW, La Pierre KJ, MacDougall AM et al. 2019. Leaf nutrients, not specific leaf area, are consistent indicators of elevated nutrient inputs. *Nature Ecology & Evolution* 3: 400–406.

Fisher JB, Sitch S, Malhi Y, Fisher RA, Huntingford C, Tan S-Y. 2010. Carbon cost of plant nitrogen acquisition: a mechanistic, globally applicable model of plant nitrogen uptake, retranslocation, and fixation. *Global Biogeochemical Cycles* 24: 2009GB003621.

Fox J, Weisberg S. 2019. *An R companion to applied regression*. London: Sage.

Franklin O, Harrison SP, Dewar R, Farrior CE, Brännström Å, Dieckmann U, Pietsch S, Falster D, Cramer W, Loreau M et al. 2020. Organizing principles for vegetation dynamics. *Nature Plants* 6: 444–453.

Franks P, Brodribb TJ. 2005. Vascular transport in plants, physiological ecology.

Frey SD. 2019. Mycorrhizal fungi as mediators of soil organic matter dynamics. *Annual Review of Ecology, Evolution, and Systematics* 50: 237–259.

Gerber S, Hedin LO, Oppenheimer M, Pacala SW, Shevliakova E. 2010. Nitrogen cycling and feedbacks in a global dynamic land model. *Global Biogeochemical Cycles* 24: 2008GB003336.

Gill AL, Finzi AC. 2016. Belowground carbon flux links biogeochemical cycles and resource-use efficiency at the global scale. *Ecology Letters* 19: 1419–1428.

Gorissen A, Jansen AE, Olsthoorn AFM. 1993. Effects of a two-year application of ammonium sulphate on growth, nutrient uptake, and rhizosphere microflora of juvenile Douglas-fir. *Plant and Soil* 157: 41–50.

Graven H, Allison CE, Etheridge DM, Hammer S, Keeling RF, Levin I, Meijer HAJ, Rubino M, Tans PP, Trudinger CM et al. 2017. Compiled records of

carbon isotopes in atmospheric CO_2 for historical simulations in CMIP6. *Geoscientific Model Development* **10**: 4405–4417.

Güsewell S. 2004. N:P ratios in terrestrial plants: variation and functional significance. *New Phytologist* **164**: 243–266.

Gutschick VP. 1981. Evolved strategies in nitrogen acquisition by plants. *American Naturalist* **118**: 607–637.

Han Y, Feng J, Han M, Zhu B. 2020. Responses of arbuscular mycorrhizal fungi to nitrogen addition: a meta-analysis. *Global Change Biology* **26**: 7229–7241.

Harpole WS, Ngai JT, Cleland EE, Seabloom EW, Borer ET, Bracken MES, Elser JJ, Gruner DS, Hillebrand H, Shurin JB et al. 2011. Nutrient co-limitation of primary producer communities. *Ecology Letters* **14**: 852–862.

Harris I, Jones PD, Osborn TJ, Lister DH. 2014. Updated high-resolution grids of monthly climatic observations – the CRU TS3 .10 Dataset. *International Journal of Climatology* **34**: 623–642.

Harrison SP, Cramer W, Franklin O, Prentice IC, Wang H, Brännström Å, De Boer H, Dieckmann U, Joshi J, Keenan TF et al. 2021. Eco-evolutionary optimality as a means to improve vegetation and land-surface models. *New Phytologist* **231**: 2125–2141.

Hartmann H, Bahn M, Carbone M, Richardson AD. 2020. Plant carbon allocation in a changing world – challenges and progress. *New Phytologist* **227**: 981–988.

Hasselquist NJ, Metcalfe DB, Högberg P. 2012. Contrasting effects of low and high nitrogen additions on soil CO_2 flux components and ectomycorrhizal fungal sporocarp production in a boreal forest. *Global Change Biology* **18**: 3596–3605.

Hawkes CV, Kivlin SN, Rocca JD, Huguet V, Thomsen MA, Suttle KB. 2011. Fungal community responses to precipitation: fungal climate response. *Global Change Biology* **17**: 1637–1645.

Hawkins H-J, Cargill RIM, Van Nuland ME, Hagen SC, Field KJ, Sheldrake M, Soudzilovskaia NA, Kiers ET. 2023. Mycorrhizal mycelium as a global carbon pool. *Current Biology* **33**: R560–R573.

Hawkins H-J, Johansen A, George E. 2000. Uptake and transport of organic and inorganic nitrogen by arbuscular mycorrhizal fungi. *Plant and Soil* **226**: 275–285.

He M, Dijkstra FA. 2014. Drought effect on plant nitrogen and phosphorus: a meta-analysis. *New Phytologist* **204**: 924–931.

van der Heijden MG, Martin FM, Selosse M-A, Sanders IR. 2015. Mycorrhizal ecology and evolution: the past, the present, and the future. *New Phytologist* **205**: 1406–1423.

Hodge A, Storer K. 2015. Arbuscular mycorrhiza and nitrogen: implications for individual plants through to ecosystems. *Plant and Soil* **386**: 1–19.

Högberg MN, Briones MJI, Keel SG, Metcalfe DB, Campbell C, Midwood AJ, Thornton B, Hurry V, Linder S, Näsholm T et al. 2010. Quantification of effects of season and nitrogen supply on tree below-ground carbon transfer to ectomycorrhizal fungi and other soil organisms in a boreal pine forest. *New Phytologist* **187**: 485–493.

Högberg MN, Högberg P, Wallander H, Nilsson L-O. 2021. Carbon–nitrogen relations of ectomycorrhizal mycelium across a natural nitrogen supply gradient in boreal forest. *New Phytologist* **232**: 1839–1848.

Högberg P, Högberg MN, Göttlicher SG, Betson NR, Keel SG, Metcalfe DB, Campbell C, Schindlbacher A, Hurry V, Lundmark T et al. 2008. High temporal resolution tracing of photosynthate carbon from the tree canopy to forest soil microorganisms. *New Phytologist* **177**: 220–228.

Hou E, Chen C, Luo Y, Zhou G, Kuang Y, Zhang Y, Heenan M, Lu X, Wen D. 2018. Effects of climate on soil phosphorus cycle and availability in natural terrestrial ecosystems. *Global Change Biology* **24**: 3344–3356.

Huber ML, Perkins RA, Laesecke A, Friend DG, Sengers JV, Assael MJ, Metaxa IN, Vogel E, Mareš R, Miyagawa K. 2009. New international formulation for the viscosity of H_2O. *Journal of Physical and Chemical Reference Data* **38**: 101–125.

Hyvönen R, Ågren GI, Linder S, Persson T, Cotrufo MF, Ekblad A, Freeman M, Grelle A, Janssens IA, Jarvis PG et al. 2007. The likely impact of elevated CO_2, nitrogen deposition, increased temperature and management on carbon sequestration in temperate and boreal forest ecosystems: a literature review. *New Phytologist* **173**: 463–480.

Jo I, Fei S, Oswalt CM, Domke GM, Phillips RP. 2019. Shifts in dominant tree mycorrhizal associations in response to anthropogenic impacts. *Science Advances* **5**: eaav6358.

Joseph J, Luster J, Bottero A, Buser N, Baechli L, Sever K, Gessler A. 2021. Effects of drought on nitrogen uptake and carbon dynamics in trees. *Tree Physiology* **41**: 927–943.

Jungk A. 2001. Root hairs and the acquisition of plant nutrients from soil. *Journal of Plant Nutrition and Soil Science* **164**: 121–129.

Kakouridis A, Hagen JA, Kan MP, Mambelli S, Feldman LJ, Herman DJ, Weber PK, Pett-Ridge J, Firestone MK. 2022. Routes to roots: direct evidence of water transport by arbuscular mycorrhizal fungi to host plants. *New Phytologist* **236**: 210–221.

Kaschuk G, Hungria M, Leffelaar PA, Giller KE, Kuyper TW. 2010. Differences in photosynthetic behaviour and leaf senescence of soybean (*Glycine max* [L.] Merrill) dependent on N2 fixation or nitrate supply: N2 fixation, photosynthesis and leaf senescence in soybean. *Plant Biology* **12**: 60–69.

Kaschuk G, Kuyper TW, Leffelaar PA, Hungria M, Giller KE. 2009. Are the rates of photosynthesis stimulated by the carbon sink strength of rhizobial and arbuscular mycorrhizal symbioses? *Soil Biology and Biochemistry* **41**: 1233–1244.

Kattge J, Diaz S, Lavorel S, Prentice IC, Leadley P, Bönisch G, Garnier E, Westoby M, Reich PB, Wright IJ. 2011. TRY–a global database of plant traits. *Global Change Biology* **17**: 2905–2935.

Keeling CD. 1998. Atmospheric CO_2 records from sites in the SIO air sampling network. In: *Trends: a compendium of data on global change*. Oak Ridge: Carbon Dioxide Information Analysis Center, Oak Ridge National Laboratory, U.S. Department of Energy.

Kjøller R, Nilsson L-O, Hansen K, Schmidt IK, Vesterdal L, Gundersen P. 2012. Dramatic changes in ectomycorrhizal community composition, root tip abundance and mycelial production along a stand-scale nitrogen deposition gradient. *New Phytologist* **194**: 278–286.

Koch KE, Johnson CR. 1984. Photosynthate partitioning in split-root citrus seedlings with mycorrhizal and nonmycorrhizal root systems. *Plant Physiology* **75**: 26–30.

Kohout P. 2017. Biogeography of ericoid mycorrhiza. In: *Biogeography of mycorrhizal symbiosis*. Cham, Switzerland: Springer International, 179–193.

Laliberté E, Lambers H, Burgess TI, Wright SJ. 2015. Phosphorus limitation, soil-borne pathogens and the coexistence of plant species in hyperdiverse forests and shrublands. *New Phytologist* **206**: 507–521.

Lambers H, Raven JA, Shaver GR, Smith SE. 2008. Plant nutrient-acquisition strategies change with soil age. *Trends in Ecology & Evolution* **23**: 95–103.

Lambers H, Shane MW, Cramer MD, Pearse SJ, Veneklaas EJ. 2006. Root structure and functioning for efficient acquisition of phosphorus: matching morphological and physiological traits. *Annals of Botany* **98**: 693–713.

Lavergne A, Sandoval D, Hare VJ, Graven H, Prentice IC. 2020. Impacts of soil water stress on the acclimated stomatal limitation of photosynthesis: insights from stable carbon isotope data. *Global Change Biology* **26**: 7158–7172.

Leadley PW, Reynolds JF, Chapin FS. 1997. A model of nitrogen uptake by *Eriophorum vaginatum* roots in the filed: ecological implications. *Ecological Monographs* **67**: 1–22.

Leake J, Johnson D, Donnelly D, Muckle G, Boddy L, Read D. 2004. Networks of power and influence: the role of mycorrhizal mycelium in controlling plant communities and agroecosystem functioning. *Canadian Journal of Botany* **82**: 1016–1045.

LeBauer DS, Treseder KK. 2008. Nitrogen limitation of net primary productivity in terrestrial ecosystems is globally distributed. *Ecology* **89**: 371–379.

Ledo A, Paul KI, Burslem DF, Ewel JJ, Barton C, Battaglia M, Brooksbank K, Carter J, Eid TH, UK JR. 2018. Tree size and climatic water deficit control root to shoot ratio in individual trees globally. *New Phytologist* **217**: 8–11.

Lefcheck JS. 2016. PIECEWISESEM: Piecewise structural equation modelling in R for ecology, evolution, and systematics. *Methods in Ecology and Evolution* **7**: 573–579.

Lehto T, Zwiazek JJ. 2011. Ectomycorrhizas and water relations of trees: a review. *Mycorrhiza* **21**: 71–90.

Leidi EO, Rodríguez-Navarro DN. 2000. Nitrogen and phosphorus availability limit N2 fixation in bean. *New Phytologist* **147**: 337–346.

Lenth RV, Bolker B, Buerkner P, Giné-Vázquez I, Herve M, Jung M, Love J, Miguez F, Riebl H, Singmann H. 2024. *Package 'emmeans'*.

Leys C, Ley C, Klein O, Bernard P, Licata L. 2013. Detecting outliers: do not use standard deviation around the mean, use absolute deviation around the median. *Journal of Experimental Social Psychology* 49: 764–766.

Leyva-Morales R, Gavito ME, Carrillo-Saucedo SM. 2019. Morphological and physiological responses of the external mycelium of Rhizophagus intraradices to water stress. *Mycorrhiza* 29: 141–147.

Lilleskov EA, Kuyper TW, Bidartondo MI, Hobbie EA. 2019. Atmospheric nitrogen deposition impacts on the structure and function of forest mycorrhizal communities: a review. *Environmental Pollution* 246: 148–162.

Lindahl BD, Tunlid A. 2015. Ectomycorrhizal fungi–potential organic matter decomposers, yet not saprotrophs. *New Phytologist* 205: 1443–1447.

Lindström K, Mousavi SA. 2020. Effectiveness of nitrogen fixation in rhizobia. *Microbial Biotechnology* 13: 1314–1335.

Liu B, Fan X, Meng D, Liu Z, Gao D, Chang Q, Bai E. 2024. Ectomycorrhizal trees rely on nitrogen resorption less than arbuscular mycorrhizal trees globally. *Ecology Letters* 27: e14346.

Madouh TA, Quoreshi AM. 2023. The function of arbuscular mycorrhizal fungi associated with drought stress resistance in native plants of arid desert ecosystems: a review. *Diversity* 15: 391.

Marklein AR, Winbourne JB, Enders SK, Gonzalez DJX, Van Huysen TL, Izquierdo JE, Light DR, Liptzin D, Miller KE, Morford SL *et al.* 2016. Mineralization ratios of nitrogen and phosphorus from decomposing litter in temperate versus tropical forests. *Global Ecology and Biogeography* 25: 335–346.

Marschner H, Dell B. 1994. Nutrient uptake in mycorrhizal symbiosis. *Plant and Soil* 159: 89–102.

Martin F, Kohler A, Murat C, Veneault-Fourrey C, Hibbett DS. 2016. Unearthing the roots of ectomycorrhizal symbioses. *Nature Reviews Microbiology* 14: 760–773.

Matimati I, Verboom GA, Cramer MD. 2014. Nitrogen regulation of transpiration controls mass-flow acquisition of nutrients. *Journal of Experimental Botany* 65: 159–168.

McDowell RW, Noble A, Pletnyakov P, Haygarth PM. 2023. A global database of soil plant available phosphorus. *Scientific Data* 10: 125.

McMurtrie RE, Dewar RC. 2013. New insights into carbon allocation by trees from the hypothesis that annual wood production is maximized. *New Phytologist* 199: 981–990.

McMurtrie RE, Näsholm T. 2018. Quantifying the contribution of mass flow to nitrogen acquisition by an individual plant root. *New Phytologist* 218: 119–130.

McNeil BE, Read JM, Driscoll CT. 2007. Foliar nitrogen responses to elevated atmospheric nitrogen deposition in nine temperate forest canopy species. *Environmental Science & Technology* 41: 5191–5197.

Medlyn BE, Duursma RA, Eamus D, Ellsworth DS, Prentice IC, Barton CVM, Crous KY, De Angelis P, Freeman M, Wingate L. 2011. Reconciling the optimal and empirical approaches to modelling stomatal conductance: reconciling optimal and empirical stomatal models. *Global Change Biology* 17: 2134–2144.

Mei L, Zhang P, Cui G, Yang X, Zhang T, Guo J. 2022. Arbuscular mycorrhizal fungi promote litter decomposition and alleviate nutrient limitations of soil microbes under warming and nitrogen application. *Applied Soil Ecology* 171: 104318.

Menge DNL, Batterman SA, Hedin LO, Liao W, Pacala SW, Taylor BN. 2017. Why are nitrogen-fixing trees rare at higher compared to lower latitudes? *Ecology* 98: 3127–3140.

Menge DNL, Levin SA, Hedin LO. 2009. Facultative versus obligate nitrogen fixation strategies and their ecosystem consequences. *American Naturalist* 174: 465–477.

Menge DNL, Wolf AA, Funk JL. 2015. Diversity of nitrogen fixation strategies in Mediterranean legumes. *Nature Plants* 1: 15064.

Mengoli G, Agustí-Panareda A, Boussetta S, Harrison SP, Trotta C, Prentice IC. 2022. Ecosystem photosynthesis in land-surface models: A first-principles approach incorporating acclimation. *Journal of Advances in Modeling Earth Systems* 14: e2021MS002767.

Meyer A, Grote R, Polle A, Butterbach-Bahl K. 2010. Simulating mycorrhiza contribution to forest C- and N cycling-the MYCOFON model. *Plant and Soil* 327: 493–517.

Midgley MG, Phillips RP. 2019. Spatio-temporal heterogeneity in extracellular enzyme activities tracks variation in saprotrophic fungal biomass in a temperate hardwood forest. *Soil Biology and Biochemistry* 138: 107600.

Montgomery D, Peck E, Vining G. 1992. *Introduction to linear regression analysis*. New York, NY, USA: John Wiley & Sons.

Mooney H. 1972. The carbon balance of plants. *Annual Review of Ecology and Systematics* 3: 315–346.

Nouri E, Matinizadeh M, Moshki A, Zolfaghari A, Rajaei S, Janoušková M. 2020. Arbuscular mycorrhizal fungi benefit drought-stressed Salsola laricina. *Plant Ecology* 221: 683–694.

Nye PH. 1977. The rate-limiting step in plant nutrient absorption from soil. *Soil Science* 123: 292–297.

Olsen SR. 1954. *Estimation of available phosphorus in soils by extraction with sodium bicarbonate*. Washington, DC: US Department of Agriculture, US Government Printing Office.

Olsson PA, Burleigh SH, Van Aarle IM. 2005. The influence of external nitrogen on carbon allocation to *Glomus intraradices* in monoxenic arbuscular mycorrhiza. *New Phytologist* 168: 677–686.

Oyewole OA, Inselsbacher E, Näsholm T. 2014. Direct estimation of mass flow and diffusion of nitrogen compounds in solution and soil. *New Phytologist* 201: 1056–1064.

Paillassa J, Wright IJ, Prentice IC, Pepin S, Smith NG, Ethier G, Westerband AC, Lamarque LJ, Wang H, Cornwell WK *et al.* 2020. When and where soil is important to modify the carbon and water economy of leaves. *New Phytologist* 228: 121–135.

Pawlowski K, Newton WE. 2007. *Nitrogen-fixing actinorhizal symbioses*. Berlin, Germany: Springer Science & Business Media.

Perkowski EA, Terrones J, German HL, Smith NG. 2024. Symbiotic nitrogen fixation reduces belowground biomass carbon costs of nitrogen acquisition under low, but not high, nitrogen availability. *AoB Plants* 16: plae051.

Perkowski EA, Waring EF, Smith NG. 2021. Root mass carbon costs to acquire nitrogen are determined by nitrogen and light availability in two species with different nitrogen acquisition strategies. *Journal of Experimental Botany* 72: 5766–5776.

Perkowski E, Smith NG. 2024. TXEco v.2.0: leaf functional trait dataset for herbaceous forb and graminoid species of Texan grasslands.

Phillips RP, Brzostek E, Midgley MG. 2013. The mycorrhizal-associated nutrient economy: a new framework for predicting carbon–nutrient couplings in temperate forests. *New Phytologist* 199: 41–51.

Phillips RP, Fahey TJ. 2006. Tree species and mycorrhizal associations influence the magnitude of rhizosphere effects. *Ecology* 87: 1302–1313.

Phillips RP, Finzi AC, Bernhardt ES. 2011. Enhanced root exudation induces microbial feedbacks to N cycling in a pine forest under long-term CO_2 fumigation. *Ecology Letters* 14: 187–194.

Poggio L, De Sousa LM, Batjes NH, Heuvelink GBM, Kempen B, Ribeiro E, Rossiter D. 2021. SoilGrids 2.0: producing soil information for the globe with quantified spatial uncertainty. *The Soil* 7: 217–240.

Poorter H, Niklas KJ, Reich PB, Oleksyn J, Poot P, Mommer L. 2012. Biomass allocation to leaves, stems and roots: meta-analyses of interspecific variation and environmental control. *New Phytologist* 193: 30–50.

Prentice IC, Dong N, Gleason SM, Maire V, Wright IJ. 2014. Balancing the costs of carbon gain and water transport: testing a new theoretical framework for plant functional ecology. *Ecology Letters* 17: 82–91.

Prescott CE. 2024. Sustaining organic matter in forest soils: what we have learned and what is left. *Soil Science Society of America Journal* 88: 1–7.

Prescott CE, Grayston SJ, Helmisaari H-S, Kaštovská E, Körner C, Lambers H, Meier IC, Millard P, Ostonen I. 2020. Surplus carbon drives allocation and plant–soil interactions. *Trends in Ecology & Evolution* 35: 1110–1118.

Pritsch K, Garbaye J. 2011. Enzyme secretion by ECM fungi and exploitation of mineral nutrients from soil organic matter. *Annals of Forest Science* 68: 25–32.

Qiao S, Wang H, Prentice IC, Harrison SP. 2020. Extending a first-principles primary production model to predict wheat yields. *Agricultural and Forest Meteorology* 287: 107932.

Querejeta JI, Allen MF, Caravaca F, Roldán A. 2006. Differential modulation of host plant δ13C and δ18O by native and nonnative arbuscular mycorrhizal fungi in a semiarid environment. *New Phytologist* 169: 379–387.

Querejeta JI, Barea JM, Allen MF, Caravaca F, Roldán A. 2003. Differential response of δ13C and water use efficiency to arbuscular mycorrhizal infection in two aridland woody plant species. *Oecologia* 135: 510–515.

Querejeta JI, Prieto I, Armas C, Casanoves F, Diémé JS, Diouf M, Yossi H, Kaya B, Pugnaire FI, Rusch GM. 2022. Higher leaf nitrogen content is linked to tighter stomatal regulation of transpiration and more efficient water use across dryland trees. *New Phytologist* 235: 1351–1364.

Querejeta JI, Egerton-Warburton LM, Allen MF. 2009. Topographic position modulates the mycorrhizal response of oak trees to interannual rainfall variability. *Ecology* 90: 649–662.

R Core Team (R, v4.3.3). 2024. *R: a language and environment for statistical computing*. Vienna, Austria: R Foundation for Statistical Computing. [WWW document] URL https://www.R-project.org/.

Raich JW, Clark DA, Schwendenmann L, Wood TE. 2014. Aboveground tree growth varies with belowground carbon allocation in a tropical rainforest environment. *PLoS ONE* 9: e100275.

Rastetter EB, Vitousek PM, Field C, Shaver GR, Herbert D, Gren GI. 2001. Resource optimization and symbiotic nitrogen fixation. *Ecosystems* 4: 369–388.

Raven JA, Lambers H, Smith SE, Westoby M. 2018. Costs of acquiring phosphorus by vascular land plants: patterns and implications for plant coexistence. *New Phytologist* 217: 1420–1427.

Read DJ. 1991. Mycorrhizas in ecosystems. *Experientia* 47: 376–391.

Read DJ, Perez-Moreno J. 2003. Mycorrhizas and nutrient cycling in ecosystems – a journey towards relevance? *New Phytologist* 157: 475–492.

Reynolds HL, Hartley AE, Vogelsang KM, Bever JD, Schultz PA. 2005. Arbuscular mycorrhizal fungi do not enhance nitrogen acquisition and growth of old-field perennials under low nitrogen supply in glasshouse culture. *New Phytologist* 167: 869–880.

Rineau F, Courty P-E. 2011. Secreted enzymatic activities of ectomycorrhizal fungi as a case study of functional diversity and functional redundancy. *Annals of Forest Science* 68: 69–80.

Roddy AB. 2023. Rethinking economic theories of plant water use. *Journal of Biosciences* 48: 21.

Rogers A, Medlyn BE, Dukes JS, Bonan G, Von Caemmerer S, Dietze MC, Kattge J, Leakey ADB, Mercado LM, Niinemets Ü *et al.* 2017. A roadmap for improving the representation of photosynthesis in Earth system models. *New Phytologist* 213: 22–42.

Ruiz-Lozano JM, Azcon R, Gomez M. 1995. Effects of arbuscular-mycorrhizal Glomus species on drought tolerance: physiological and nutritional plant responses. *Applied and Environmental Microbiology* 61: 456–460.

Ruth B, Khalvati M, Schmidhalter U. 2011. Quantification of mycorrhizal water uptake via high-resolution on-line water content sensors. *Plant and Soil* 342: 459–468.

Salazar-Tortosa D, Castro J, Villar-Salvador P, Viñegla B, Matías L, Michelsen A, Rubio De Casas R, Querejeta JI. 2018. The "isohydric trap": A proposed feedback between water shortage, stomatal regulation, and nutrient acquisition drives differential growth and survival of European pines under climatic dryness. *Global Change Biology* 24: 4069–4083.

Schielzeth H, Dingemanse NJ, Nakagawa S, Westneat DF, Allegue H, Teplitsky C, Réale D, Dochtermann NA, Garamszegi LZ, Araya-Ajoy YG. 2020. Robustness of linear mixed-effects models to violations of distributional assumptions. *Methods in Ecology and Evolution* 11: 1141–1152.

See CR, Keller AB, Hobbie SE, Kennedy PG, Weber PK, Pett-Ridge J. 2022. Hyphae move matter and microbes to mineral microsites: integrating the hyphosphere into conceptual models of soil organic matter stabilization. *Global Change Biology* 28: 2527–2540.

Shah F, Nicolás C, Bentzer J, Ellström M, Smits M, Rineau F, Canbäck B, Floudas D, Carleer R, Lackner G. 2016. Ectomycorrhizal fungi decompose soil organic matter using oxidative mechanisms adapted from saprotrophic ancestors. *New Phytologist* 209: 1705–1719.

Sheldon ND, Smith SY, Stein R, Ng M. 2020. Carbon isotope ecology of gymnosperms and implications for paleoclimatic and paleoecological studies. *Global and Planetary Change* 184: 103060.

Shi J, Wang X, Wang E. 2023. Mycorrhizal symbiosis in plant growth and stress adaptation: From genes to ecosystems. *Annual Review of Plant Biology* 74: 569–607.

Shi M, Fisher JB, Brzostek ER, Phillips RP. 2016. Carbon cost of plant nitrogen acquisition: global carbon cycle impact from an improved plant nitrogen cycle in the Community Land Model. *Global Change Biology* 22: 1299–1314.

Smith NG. 2024. Opportunities to improve our understanding of the impact of photosynthetic acclimation on terrestrial ecosystem processes under global change. *American Journal of Botany* 111: e16313.

Smith NG, Keenan TF. 2020. Mechanisms underlying leaf photosynthetic acclimation to warming and elevated CO_2 as inferred from least-cost optimality theory. *Global Change Biology* 26: 5202–5216.

Smith NG, Keenan TF, Colin Prentice I, Wang H, Wright IJ, Niinemets Ü, Crous KY, Domingues TF, Guerrieri R, Yoko Ishida F *et al.* 2019. Global photosynthetic capacity is optimized to the environment. *Ecology Letters* 22: 506–517.

Smith SE, Read DJ. 2010. *Mycorrhizal symbiosis*. New York, NY, USA: Academic Press.

Soudzilovskaia NA, Douma JC, Akhmetzhanova AA, Van Bodegom PM, Cornwell WK, Moens EJ, Treseder KK, Tibbett M, Wang Y, Cornelissen JHC. 2015. Global patterns of plant root colonization intensity by mycorrhizal fungi explained by climate and soil chemistry. *Global Ecology and Biogeography* 24: 371–382.

Soudzilovskaia NA, Vaessen S, Barcelo M, He J, Rahimlou S, Abarenkov K, Brundrett MC, Gomes SI, Merckx V, Tedersoo L. 2020. FungalRoot: global online database of plant mycorrhizal associations. *New Phytologist* 227: 955–966.

Soudzilovskaia NA, Van Bodegom PM, Terrer C, Zelfde MV, McCallum I, Luke McCormack M, Fisher JB, Brundrett MC, De Sá NC, Tedersoo L. 2019. Global mycorrhizal plant distribution linked to terrestrial carbon stocks. *Nature Communications* 10: 5077.

Sperry JS, Venturas MD, Anderegg WR, Mencuccini M, Mackay DS, Wang Y, Love DM. 2017. Predicting stomatal responses to the environment from the optimization of photosynthetic gain and hydraulic cost. *Plant, Cell & Environment* 40: 816–830.

Stocker BD, Wang H, Smith NG, Harrison SP, Keenan TF, Sandoval D, Davis T, Prentice IC. 2020. P-model v1.0: an optimality-based light use efficiency model for simulating ecosystem gross primary production. *Geoscientific Model Development* 13: 1545–1581.

Stocker BD, Zscheischler J, Keenan TF, Prentice IC, Peñuelas J, Seneviratne SI. 2018. Quantifying soil moisture impacts on light use efficiency across biomes. *New Phytologist* 218: 1430–1449.

Sullivan BW, Smith WK, Townsend AR, Nasto MK, Reed SC, Chazdon RL, Cleveland CC. 2014. Spatially robust estimates of biological nitrogen (N) fixation imply substantial human alteration of the tropical N cycle. *Proceedings of the National Academy of Sciences, USA* 111: 8101–8106.

Talbot JM, Allison SD, Treseder KK. 2008. Decomposers in disguise: mycorrhizal fungi as regulators of soil C dynamics in ecosystems under global change. *Functional Ecology* 22: 955–963.

Tedersoo L, Bahram M. 2019. Mycorrhizal types differ in ecophysiology and alter plant nutrition and soil processes. *Biological Reviews* 94: 1857–1880.

Tedersoo L, Brundrett MC. 2017. Evolution of ectomycorrhizal symbiosis in plants. In: *Biogeography of mycorrhizal symbiosis*, Cham, Switzerland: Springer, 407–467.

Tedersoo L, Laanisto L, Rahimlou S, Toussaint A, Hallikma T, Pärtel M. 2018. Global database of plants with root-symbiotic nitrogen fixation: Nod DB. *Journal of Vegetation Science* 29: 560–568.

Tedersoo L, Smith ME. 2013. Lineages of ectomycorrhizal fungi revisited: Foraging strategies and novel lineages revealed by sequences from belowground. *Fungal Biology Reviews* 27: 83–99.

Terrer C, Vicca S, Hungate BA, Phillips RP, Prentice IC. 2016. Mycorrhizal association as a primary control of the CO_2 fertilization effect. *Science* 353: 72–74.

Terrer C, Vicca S, Stocker BD, Hungate BA, Phillips RP, Reich PB, Finzi AC, Prentice IC. 2018. Ecosystem responses to elevated CO_2 governed by plant–soil interactions and the cost of nitrogen acquisition. *New Phytologist* 217: 507–522.

Teste FP, Jones MD, Dickie IA. 2020. Dual-mycorrhizal plants: their ecology and relevance. *New Phytologist* 225: 1835–1851.

Thomas RQ, Brookshire ENJ, Gerber S. 2015. Nitrogen limitation on land: how can it occur in Earth system models? *Global Change Biology* 21: 1777–1793.

Thoning KW, Tans PP, Komhyr WD. 1989. Atmospheric carbon dioxide at Mauna Loa Observatory: 2. Analysis of the NOAA GMCC data, 1974–1985. *Journal of Geophysical Research: Atmospheres* 94: 8549–8565.

Treseder KK. 2004. A meta-analysis of mycorrhizal responses to nitrogen, phosphorus, and atmospheric CO_2 in field studies. *New Phytologist* 164: 347–355.

Treseder KK, Allen MF. 2000. Mycorrhizal fungi have a potential role in soil carbon storage under elevated CO_2 and nitrogen deposition. *New Phytologist* 147: 189–200.

Turner BL, Brenes-Arguedas T, Condit R. 2018. Pervasive phosphorus limitation of tree species but not communities in tropical forests. *Nature* 555: 367–370.

Ubierna Lopez N, Farquhar G. 2014. Advances in measurements and models of photosynthetic carbon isotope discrimination in C3 plants. *Plant, Cell & Environment* 37: 365–381.

Udvardi M, Poole PS. 2013. Transport and metabolism in legume-rhizobia symbioses. *Annual Review of Plant Biology* 64: 781–805.

Valentine HT, Mäkelä A. 2012. Modeling forest stand dynamics from optimal balances of carbon and nitrogen. *New Phytologist* 194: 961–971.

Vallicrosa H, Sardans J, Maspons J, Zuccarini P, Fernández-Martínez M, Bauters M, Goll DS, Ciais P, Obersteiner M, Janssens IA *et al.* 2022. Global maps and factors driving forest foliar elemental composition: the importance of evolutionary history. *New Phytologist* 233: 169–181.

Vance CP, Heichel GH. 1991. Carbon in N_2 fixation: limitation or exquisite adaptation. *Annual Review of Plant Physiology and Plant Molecular Biology* 42: 373–390.

Vance CP, Uhde-Stone C, Allan DL. 2003. Phosphorus acquisition and use: critical adaptations by plants for securing a nonrenewable resource. *New Phytologist* 157: 423–447.

Vitousek PM. 2004. *Nutrient cycling and limitation: Hawai'i as a model system.* Princeton, NJ, USA: Princeton University Press.

Vitousek PM, Menge DN, Reed SC, Cleveland CC. 2013. Biological nitrogen fixation: rates, patterns and ecological controls in terrestrial ecosystems. *Philosophical Transactions of the Royal Society, B: Biological Sciences* 368: 20130119.

Vitousek PM, Porder S, Houlton BZ, Chadwick OA. 2010. Terrestrial phosphorus limitation: mechanisms, implications, and nitrogen–phosphorus interactions. *Ecological Applications* 20: 5–15.

Vitousek PM, Howarth RW. 1991. Nitrogen limitation on land and in the sea: how can it occur? *Biogeochemistry* 13: 87–115.

Vohník M. 2020. Ericoid mycorrhizal symbiosis: theoretical background and methods for its comprehensive investigation. *Mycorrhiza* 30: 671–695.

Wallander H, Nylund J-E. 1992. Effects of excess nitrogen and phosphorus starvation on the extramatrical mycelium of ectomycorrhizas of *Pinus sylvestris* L. *New Phytologist* 120: 495–503.

Wang H, Prentice IC, Davis TW, Keenan TF, Wright IJ, Peng C. 2017a. Photosynthetic responses to altitude: an explanation based on optimality principles. *New Phytologist* 213: 976–982.

Wang H, Prentice IC, Keenan TF, Davis TW, Wright IJ, Cornwell WK, Evans BJ, Peng C. 2017b. Towards a universal model for carbon dioxide uptake by plants. *Nature Plants* 3: 734–741.

Wang J, Zhang H, Gao J, Zhang Y, Liu Y, Tang M. 2021. Effects of ectomycorrhizal fungi (*Suillus variegatus*) on the growth, hydraulic function, and non-structural carbohydrates of *Pinus tabulaeformis* under drought stress. *BMC Plant Biology* 21: 171.

Wang R, Cavagnaro TR, Jiang Y, Keitel C, Dijkstra FA. 2021. Carbon allocation to the rhizosphere is affected by drought and nitrogen addition. *Journal of Ecology* 109: 3699–3709.

Wang R, Lu J, Jiang Y, Dijkstra FA. 2022. Carbon efficiency for nutrient acquisition (CENA) by plants: role of nutrient availability and microbial symbionts. *Plant and Soil* 476: 289–300.

Weedon GP, Balsamo G, Bellouin N, Gomes S, Best MJ, Viterbo P. 2014. The WFDEI meteorological forcing data set: WATCH Forcing Data methodology applied to ERA-Interim reanalysis data. *Water Resources Research* 50: 7505–7514.

Wen Z, White PJ, Shen J, Lambers H. 2022. Linking root exudation to belowground economic traits for resource acquisition. *New Phytologist* 233: 1620–1635.

Wolfe BE, Tulloss RE, Pringle A. 2012. The irreversible loss of a decomposition pathway marks the single origin of an ectomycorrhizal symbiosis. *PLoS ONE* 7: e39597.

Wright IJ, Reich PB, Westoby M. 2003. Least-cost input mixtures of water and nitrogen for photosynthesis. *The American Naturalist* 161: 98–111.

Yin H, Wheeler E, Phillips RP. 2014. Root-induced changes in nutrient cycling in forests depend on exudation rates. *Soil Biology and Biochemistry* 78: 213–221.

Yuan ZY, Chen HYH. 2012. A global analysis of fine root production as affected by soil nitrogen and phosphorus. *Proceedings of the Royal Society B: Biological Sciences* 279: 3796–3802.

Zhang F, Zou Y-N, Wu Q-S. 2018. Quantitative estimation of water uptake by mycorrhizal extraradical hyphae in citrus under drought stress. *Scientia Horticulturae* 229: 132–136.

Zomer RJ, Xu J, Trabucco A. 2022. Version 3 of the Global Aridity Index and potential evapotranspiration database. *Scientific Data* 9: 409.

Supporting Information

Additional Supporting Information may be found online in the Supporting Information section at the end of the article.

Fig. S1 Location of sites where the leaf stable carbon isotopes measurements used in this study were sampled, overlaid on the Whittaker biome classification system.

Fig. S2 Global distribution of the sites where the leaf stable carbon isotopes measurements used in this study were sampled.

Fig. S3 Graphical representation of the structural equation model used to test the direct effects of moisture index (MI) on soil nutrient availability, as well as the effects of the MI, soil nutrient availability, and soil resource acquisition strategies on β.

Fig. S4 Estimated natural-log-transformed β values against carbon isotope fractionation in leaves ($\Delta^{13}C_{leaf}$), and isotope-derived $\chi_{isotopes}$.

Fig. S5 Natural-log-transformed β values against natural-log-transformed soil N : C ratios, the square root of moisture index, and the natural-log-transformed plant-available soil P_i.

Fig. S6 Natural-log-transformed nitrogen-to-carbon ratios and soil soluble plant-available phosphorus concentration for temperate and boreal biomes and tropical and subtropical biomes.

Notes S1 Photorespiratory compensation point Γ^* and Michaelis–Menten coefficients of photosynthesis.

Notes S2 Soil data.

Table S1 Regression coefficients for the linear mixed-effects model with β as the dependent variable.

Please note: Wiley is not responsible for the content or functionality of any Supporting Information supplied by the authors. Any queries (other than missing material) should be directed to the *New Phytologist* Central Office.